UNIVERSITÀ DEGLI STUDI DI TRENTO

Dipartimento di Ingegneria Civile Ambientale Meccanica

EXPERIMENTAL AND NUMERICAL ANALYSES OF THE LOADING RATE INFLUENCE ON THE T-STUB RESPONSE

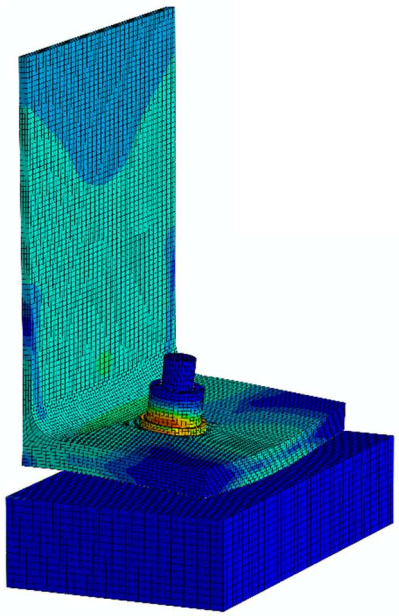

Nadia Baldassino, Martina Bernardi, Riccardo Zandonini

ISBN (online) 978-88-8443-755-6
DOI 10.15168/11572_219182

Publisher: Università degli Studi di Trento, via Calepina, 14 – 38122 Trento

Title: Experimental and numerical analyses of the loading rate influence on the T-stub response

September 2017

Authors: Nadia Baldassino, Martina Bernardi, Riccardo Zandonini

EXPERIMENTAL AND NUMERICAL ANALYSES OF THE LOADING RATE INFLUENCE ON THE T-STUB RESPONSE

Nadia Baldassino, Martina Bernardi, Riccardo Zandonini
nadia.baldassino@unitn.it, martina.bernardi@unitn.it, riccardo.zandonini@unitn.it
Department of Civil, Environmental and Mechanical Engineering
University of Trento

Abstract

The joints ductility plays a central role in ensuring a robust performance of structures by preventing progressive collapses of steel and steel-concrete composite frames subjected to accidental actions. With reference to the steel and steel-concrete frames, the connections response is well approximated by the "component method", codified also by the Eurocode 3 part 1-8. The column flange and the end-plate are the components that influence the most the rotation capacity and the ductility of an end-plate beam-to-column joint. These components are well modelled by using equivalent "T-stub" elements. The T-stubs response when subjected to quasi-static tensile loadings has been widely investigated over the years. On the contrary, the studies concerning their performance when subjected to tensile loadings with higher loading rates are, at present, quite limited. Nevertheless, the dynamic nature of the phenomena associated to the accidental actions on the structures is apparent. This factor calls for ensuring local joint ductility under dynamic forces. Therefore, deepening the knowledge of the T-stub performance under increasing loading rates is important. In the framework of the "RobustImpact" European project this topic was investigated. The study was carried out both experimentally and numerically. T-stub elements were "extracted" from the end-plate and the column flange of the beam-to-column joints of composite frames tested under the column loss scenario. Twenty specimens were tested under different displacement rates. In addition, the corresponding numerical models were developed and calibrated using the FE commercial software *Abaqus*. This document presents the experimental and numerical analyses and their main outcomes.

Index

1 Introduction

Recent studies of structural robustness pointed out the key role of local ductility, and in particular of beam-to-column joints, to prevent progressive collapse of steel and steel-concrete composite structures [1]. A structure can be defined robust if it is able to withstand local damages caused by accidental events like fire, explosions, impacts or consequences of human error without being damaged to an extent disproportionate to the original cause. When damage is associated with a column collapse, this requirement implies that an alternated load path can be established. This requires that catenary actions can develop in the beams characterized by large displacements and deformations. Therefore a structure should be designed in order to enable the activation of catenary actions involving the undamaged part of the building, since these actions would reduce the extent of the damaged portion of the structure. Within this design philosophy, the structural elements and, especially, the joints should have adequate load-bearing and deformation capacity. As to the steel and steel-concrete frames, the beam-to-column joints behaviour is well modelled by means of the "component method". According to this method, a joint can be seen as an assembly of basic components, whose stiffness and strength properties allow the overall response of the joint to be approximated. The rotational capacity of the steel connections depends on the more ductile components. In the case of bolted beam-to-column joints a significant part of the plastic rotation is provided by two components: the end-plate and the column flange. The behaviour of both of them is well approximated by equivalent "T-stubs" elements ([2] [3] [4]). Being the T-stubs the main sources of ductility of the joints in tension, the knowledge of the T-stubs response, in terms of load-displacement curve, enables evaluation of the plastic rotational capacity of the beam-to-column joints.

Most of the available experimental studies of structural progressive collapse have been performed in quasi static conditions. Nevertheless, these conditions don't represent the actual conditions under accidental loads damaging a structure. As a matter of fact, the dynamic nature of the phenomena associated with the accidental actions should, in principle, be accounted for. In other terms the question arises about the significance of the loading rate. Material strain rate sensitivity has been widely investigated in the past ([5] [6]). The knowledge of the strain rate influence on structural behaviour is, on the contrary, quite limited [7]. Consistently, the response of steel joints and of their components, such as the T-stubs, under static and cyclic loadings has been extensively investigated. Whereas, the performance of joints and of their components under dynamic loadings received modest attention. The need of further studies concerning the strain rate influence on the connections is, therefore, apparent. This need was recognized in the European research project "RobustImpact", in which the University of Trento was recently involved. The project was focused on the development of new design concepts for steel-concrete composite frames subjected to accidental actions. Two full-scale subframes were tested under the column loss scenario [8]. In the framework of the experimental activities, the influence of the loading rate on the beam-to-column joint performance was also investigated [9]. The study comprised tensile tests on T-stubs modelling the flush end-plate beam-to-column bolted connection adopted for the frame specimens. Both the column flange and the end-plate T-stubs responses were investigated subjected to different displacement rates. A numerical model has then been developed with the commercial software *Abaqus* [10] introducing "solid 3D" elements, in order to simulate these tensile tests on the T-stubs. The numerical model has been validated against experimental results. In this paper the experimental and the numerical analyses performed and their outcomes are presented.

2 The structural robustness and the RobustImpact project

When a structure undergoes accidental loadings it could be damaged and some local failures could occur. This localized damage can result in the progressive collapse ([11] [12]) of an extended part or the whole structure, when the structure itself hasn't got adequate resources in terms of strength, ductility, stability, continuity and redundancy. Such a spread of damages can be prevented, if the structure is able to transfer the loads from its damaged part to the undamaged ones. Progressive collapse under accidental actions is relatively rare, nevertheless the huge economic and lives losses associated with this kind of events require the design of "robust" structures. The recent studies of the structural robustness made most design standards ([13] [14] [15] [16]) to consider the robustness as a structural design requirement, in addition to the "traditional" ones. The joints play a key role in the structures behaviour in case of accidental actions, since they enable an alternative load path to be activated, ensuring to the structure the vital continuity and ductility. Their accurate characterization is therefore necessary to understand the structures behaviour during and after the accidental events [18], and to develop then reliable design rules.

2.1 The RobustImpact project

The European research project "RobustImpact – Robust impact design of steel and composite building structures" (RFSR-CT-2012-00029) aimed to develop a new design approach for framed steel and steel-concrete composite structures subjected to impact loads, based on the combination of two design methods, i.e. the "residual strength method" and the "alternate load path method" [8].

The research project comprised of a substantial experimental programme, dealing with all the key aspects of the response under impact loading from the local to the global issues. The research group of the University of Trento contributed by testing two 3D full scale sub-frames and, as mentioned above, a series of T-stubs. All the sub-structures and structural elements tested were part of a unique reference structure [8]: a 3D composite frame designed according to the Eurocodes ([19] [20]). This case study was a typical five-storey steel-concrete composite structure, characterized by bolted flush-end plate beam-to-column connections, fixed connections at the base, a concrete solid slab and full strength headed stud shear connections between the beams and the concrete slab.

3 The T-stubs and the strain rate sensitivity

3.1 The component method

The analysis of steel joints is usually carried out by means of the so-called "component method", as codified by the EN 1993-1-8 code [21]. As to the end-plate connections, this approach was first proposed by Yee and Melchers [22]. This method permits to obtain the moment-rotation curve of a bolted beam-to-column connection, considering the possible deformations and the ultimate capacity (and collapse modes) of each one of the components of the connection. Yee and Melchers recognized that the overall stiffness of the joint is the result of the following set of individual contributions:

- flexural deformation of the end-plate;
- flexural deformation of the column flange;
- bolt extension;
- shear deformation of the panel zone;

- deformation due to the zone of the column web in compression.

The ultimate moment capacity of the connection is determined by the weakest element.

The key point of the component method, whose roots can be identified in the Yee and Melchers paper, is considering the connection as a set of single basic components. Each component will be modelled as a linear spring characterized by its stiffness and strength in tension, compression or shear.

The implementation of the component method requires the following steps:

- the identification of the "active components" of the connection;
- the evaluation of the mechanical characteristics of every component (e.g. elastic stiffness, design resistance, plastic deformation capacity [21]);
- the assembly of the components, in order to obtain the overall connection response (e.g. in terms of initial stiffness, design resistance, moment-rotation curve).

As previously pointed out, the EN 1993-1-8 [21] adopted and codified the component method.

The study and the modelling of the end-plate connections lead to the introduction of T elements (the so-called "T-stubs"). As an example, in Figure 1 the recognizable T-stubs in an unstiffened bolted extended end-plate connection are represented.

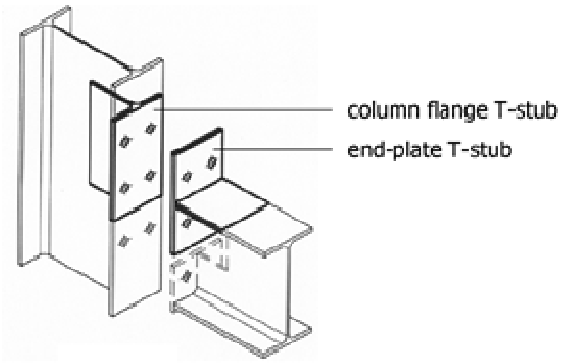

Figure 1: T-stub identification for an unstiffened bolted extended end-plate connection

3.2 The T-stubs

A T-stub element is comprised of a web and a flange bolted to a rigid support [2]. When subject to a tensile force, the web is stressed in tension, the flange in shear and bending and the bolts in tension and bending. This element is versatile, enabling modelling the response of a variety of connection components from end-plate to angle cleated connections. Its failure modes are associated with the plastic mechanisms of the flange and the strength of the bolts. Therefore, an adequate identification of the failure mechanism of the T-stub flange-bolt system is of paramount importance for predicting its performance. On the basis of extensive studies carried out all over the years ([2] [3] [4]), three failure mechanisms have been identified. These three failure mechanisms are associated to the collapse modes called mode 1, mode 2 and mode 3, as depicted in Figure 2 and described hereafter; these collapse modes are also codified in the Eurocode [21].

In collapse mode 1, a plastic mechanism develops with four yield lines. Collapse mode 2 is characterised by the formation of two plastic hinges and bolts fracture, due to the increase of bolts internal actions because of the prying forces. The collapse mode 3 is characterized by the bolts fracture.

The smallest load between those associated with each one of the three collapse modes defines the T-stub collapse load.

Different components can be simulated by means of an equivalent T-stub of a suitable 'effective' length l_{eff} [21]. The effective length is defined on the basis of strength equivalence between the component to be simulated and the T-stub model. The equivalent T-stub concept enables simulating the tensile response of basic components such: column flange in bending, end-plate in bending, flange cleat in bending and base plate in bending. Similarly, an equivalent T-stub in compression may be used to model the following basic components: the steel base plate in bending and the concrete and/or grout joint material in bearing.

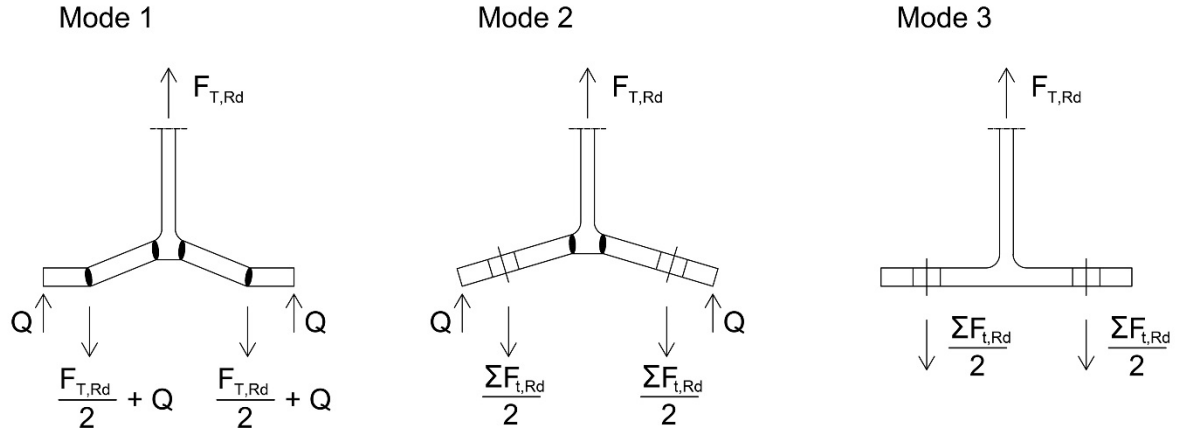

Figure 2: The three collapse modes, as identified by EN 1993-1-8 [21]

3.3 The strain rate sensitivity

The influence of the strain rate on the materials behaviour is well known, and many constitutive models have been developed over the years accounting for this influence in their formulations ([5] [6]). The studies of the strain rate influence on the joints response are quite limited, even though its importance has been recognized [23]. Furthermore, the material strain rate sensitivity has yet to be considered in the assessment of the structural robustness, despite its potential key role [7]. Recently, Pereira [7] demonstrated experimentally and numerically that the effects of the rate sensitivity, for moderate rates such as the ones induced by a gravity-driven event (e.g. sudden column loss), are less important at the component level than at the material level. However, it should be noticed that different joints geometrical or material configurations other than those studied by Pereira might present higher rate-sensitivity.

3.3.1 The material strain rate sensitivity

The strain rate is defined as the deformation that a material is subjected to per time unit. The properties of many ductile materials depend on the loading rate. For example, the mild steel plastic behaviour is highly strain rate sensitive. As a result, many constitutive equations has been developed in order to take the rate-sensitivity into account, though big efforts are needed for the parameters determination ([24] [25]). The Cowper-Symonds relationship was here adopted. In literature, the great variability of its relevant parameters is pointed out [24]. Furthermore, the experimental coupons characteristics (e.g. in terms of surface and heat treatments and chemical composition) can remarkably affect the experimental outcomes. For these reasons, a reliable characterization of the material is essential. In this study, the parameters were obtained from a set of dynamic tests carried out on the structural steel of the T-stubs (Appendix A, Paragraph 8.3).

3.4 The T-stubs subjected to dynamic loadings: the state of the art

In the last decades, various experimental analyses were carried out of the T-stubs subjected to static ([26] [27]) and cyclic loadings [28], for the seismic design of structures. The knowledge of T-stubs response, and more generally of joints, under dynamic loadings is still limited. The available studies of T-stubs subjected to dynamic loadings can be classified as moderate rate tests and impact tests.

3.4.1 Moderate rate tests

A series of tests on T-stubs subjected to different loading rates was carried out at the University of Trento in 2012, in the framework of a research project coordinated by the Imperial College of London ([7] [29]). The following parameters were varied: end-plate geometry, bolts characteristics, structural steel and welds characteristics. The tests were performed mainly quasi-statically (0,07 mm/s) or with a moderate rate typical of a gravity driven scenario (40,00 mm/s), such as in the case of a column loss in a building. A limited number of tests were also carried out at higher rates. For the geometries and steel tested, the results pointed out that the rate effects are less significant at components level than at material levels. This could be due to the fact that the plasticity spread was not enough to activate a significant dynamic over-strength [7].

3.4.2 Impact tests

Within the research project “Impactfire”, a set of tests on T-stubs subjected to impact loadings was performed at the University of Coimbra, in order to evaluate their behaviour and the strain rate influence. The outcomes pointed out an increase of the plastic resistance of the T-stubs, with smaller displacements in the case of dynamic tests, if compared with the quasi-static outcomes. It was observed that the plastic resistance increase is less important for stiffer T-stubs, characterized by collapse mode 3. In addition to the experimental tests, also analytical and numerical models were developed. The numerical and parametrical studies led to the conclusion that less ductile collapse modes are activated by higher deformation rates [31].

4 The experimental programme – the tests on the T-stubs

As mentioned in the above, the experimental part of the study presented in this document concerned the investigation of the influence of the loading rate on the response of the beam-to-column joints of the reference frame of the ‘Robustimpact’ project. Two key components of the joints were investigated: the column flange and the end-plate in bending. Twenty tensile tests on unstiffened T-stubs were carried out [32]: ten tests on end-plate T-stubs and ten on the column flange T-stubs. Two different displacement rates were considered, and quasi-static tests were also performed for comparison.

In addition, a series of tensile tests on the bolts and on the structural steel of the T-stubs was done in order to reach a proper characterization of each factor. The results of these complementary tests are reported in the experimental Appendix A (Paragraphs 8.2 and 8.3).

4.1 The specimens layout

The joints (Figure 3 and Figure 4) of the reference structure were designed according to the EN 1993-1-8 [21] and EN 1994-1-1 [20] codes (Paragraph 2.1).

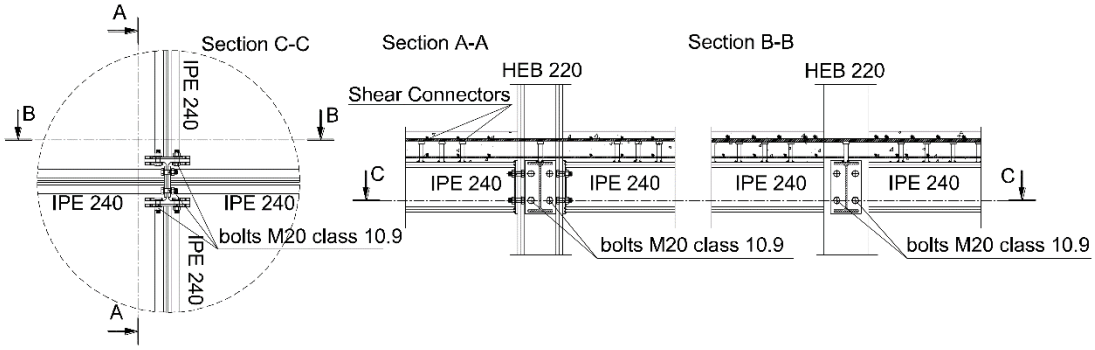

Figure 3: Steel-concrete composite joint of the reference structure

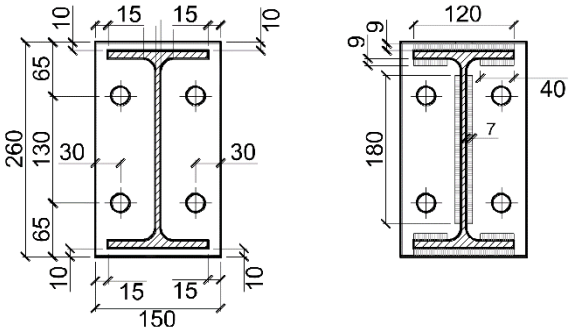

Figure 4: Detail of the beam-to-column steel connection (measures in mm): position of the beam (on the left) and main dimensions of the welds (on the right)

In the design, the nominal geometrical dimensions and the nominal mechanical properties were considered for the structural steel (S355) and for the bolts (M20 grade 10.9). A detailed description of the T-stub geometry, as obtained from the design analysis is given in Figure 5. As previously pointed out, both the end-plate and the column flange specimens were considered. An important difference between the two series lies in the thickness: 16 mm for the column flange T-stubs vs. 10 mm for the end-plate T-stubs. In addition, the two series of T-stubs are characterized by a different position of the bolts respect to the edge of the T-stubs flanges and by different lengths, which are the “equivalent” lengths of the T-stubs.

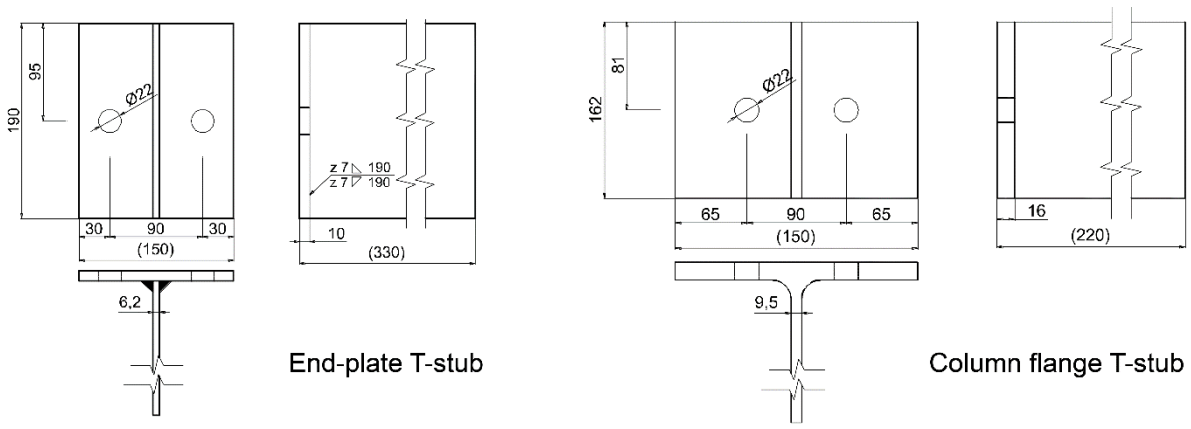

Figure 5: T-stubs geometry: end-plate and column flange T-stubs (measures in mm)

In Table 1 the results of the design analysis in accordance with the Eurocode 3 recommendations [21] are reported, in terms of “equivalent” length, collapse load and collapse mode. The expected collapse modes

are: mode 2 (with bolts failure and flange yielding) for the column flange T-stubs and mode 1 (with complete flange yielding) for the end-plate T-stubs (Section 3.2, Figure 2). The values of the collapse loads reported in Table 1, have been calculated according to the so-called Method 1 of Eurocode 3 [21], in which the force applied to the T-stub flange by a bolt is assumed to be concentrated at the centre-line of the bolt.

Joint component	Effective length mm	Collapse mode	Collapse load kN
End-plate	190	mode 1	186,38
Column flange	162	mode 2	344,77

Table 1: Theoretical effective length, collapse loads and modes for the T-stubs

Before the testing phase, the geometrical dimensions of the T-stubs, the bolts, the nuts and the washers were measured, in order to point out the possible dimensional deviation with respect to the nominal values. The mean effective dimensions were then also adopted in the numerical analyses (Section 5.1).

4.2 The testing rig and the instruments set-up

A global view of the testing rig is reported in Figure 6. It consists of a MTS actuator, with a maximum capacity in tension and compression of 1000 kN and a maximum displacement rate of 326,90 mm/s, connected, at the midspan of the upper girder, to a closed frame. At its lower end a hydraulic fixture was bolted, which was holding by friction the web plate of the T-stubs. The flange of the specimens were bolted to a rigid support, connected to the bottom midspan of the rigid frame. The tensile tests were performed in displacement control and the load was applied through the web of the T-stub, so as the force was concentric to the bolts connecting the flange to the rigid support. These two bolts were preloaded with a torque moment of 0,55 kNm, in order to achieve consistency with the bolts preloading adopted for the 3D tests on the full-scale specimens [8].

Figure 6: The testing rig and a T-stub set for the test

In order to evaluate the specimens deformation capacity, i.e. the displacement of the flange, during the tests, a set of three displacement transducers was provided. The transducers were placed under the flange of the T-stubs at three different locations along the specimen web, as illustrated in Figure 7. Moreover, all the bolts

were instrumented with internal strain gauges (Figure 7), that enabled measure of the shank elongation. In order to evaluate the force acting on the bolts and consequently to get information on the prying effects, each bolt was calibrated before the installation (Figure 8). The calibration, carried out in the elastic range, permitted to identify a "calibration curve" in terms of force vs. axial strain relationship, specific for each individual bolt (Figure 8).

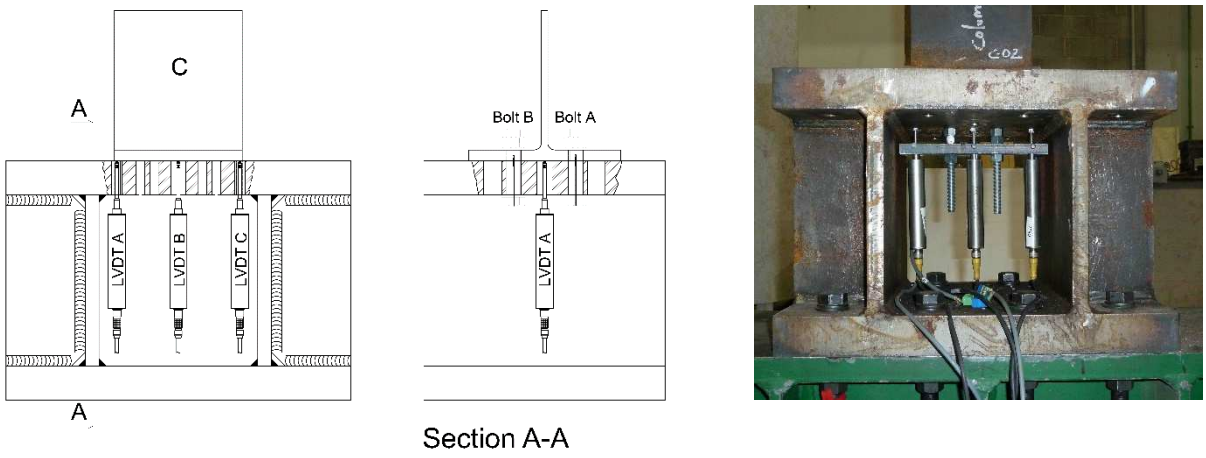

Figure 7: The instruments set-up

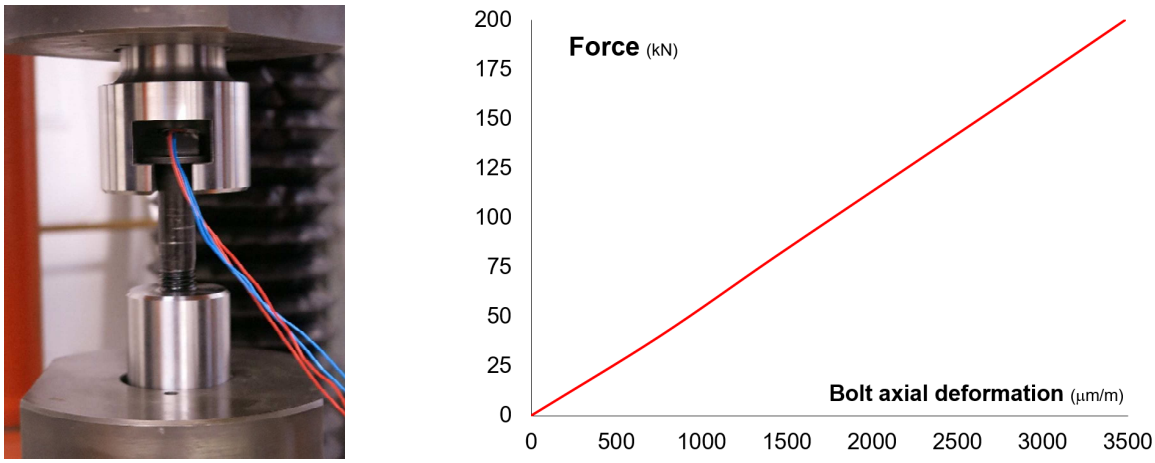

Figure 8: A bolt during the calibration phase and a typical calibration curve

During the tests, the load, the displacements and the bolts axial deformation were automatically recorded at a frequency of 4800 Hz. In case of quasi-static tests, the acquisition frequency was reduced to 200 Hz.
In order to fully characterize the behaviour of the bolts and the structural steel of the assemblies, tensile tests on both the bolts assemblies (constituted by the bolt, the nut and two washers) and the steel coupons were performed at different loading rates (Paragraphs 8.2 and 8.3). The data obtained from these tensile tests were used in the subsequent numerical analyses (Paragraph 5).

4.3 The loading protocol

The specimens were subjected to monotonic tensile tests, carried out under displacement control. Aiming at the evaluation of the loading rate influence on the T-stub performance, tests were carried out with two different levels of displacement rate (160,00 mm/s and 326,90 mm/s).

Higher displacement rates were not possible due to actuator features. For each type of T-stub, the experimental programme included three tests for each considered displacement rate. Besides, for comparison purpose, three quasi-static tests were carried out at a displacement rate of 0,07 mm/s. The tenth specimen of each T-stub series was used as a reserve.

The T-stub loading time-history is plotted in Figure 9. An initial cycle of loading and unloading, well within the elastic range, aimed to eliminate any lack of fit. This loading and unloading cycle was followed by a first ramp of loading at low displacement rate (i.e. 0,07 mm/s), giving the actuator sufficient inertia for the subsequent high rate loading ramp (characterized by the displacement rate $\dot{\delta}$).

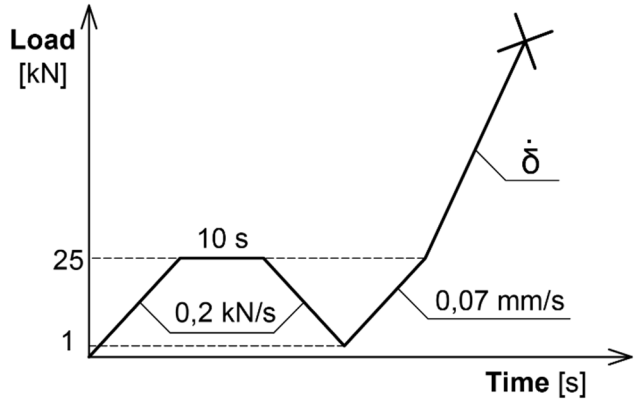

Figure 9: Typical loading history (graph not in scale)

The main characteristics of the tests undertaken, with the related loading conditions (represented by the bolts preload and the displacement rate $\dot{\delta}$ (Figure 9)), are reported in Table 2.

COLUMN FLANGE T-STUBS			END-PLATE T-STUBS		
Spec. ID	**Bolts preload torque moment** kNm	**Disp. rate $\dot{\delta}$** mm/s	**Spec. ID**	**Bolts preload torque moment** kNm	**Disp. rate $\dot{\delta}$** mm/s
C-01	0,55	326,90	EP-01	0,55	326,90
C-02	0,55	326,90	EP-02	0,55	326,90
C-03	0,55	326,90	EP-03	0,55	326,90
C-04	Preliminary test		EP-04	0,55	0,07
C-05	0,55	0,07	EP-05	0,55	0,07
C-06	0,55	0,07	EP-06	0,55	0,07
C-07	0,55	0,07	EP-07	0,55	160,00
C-08	0,55	160,00	EP-08	0,55	160,00
C-09	0,55	160,00	EP-09	0,55	160,00
C-10	0,55	160,00	EP-10	Snug tightened	160,00

Table 2: The tested column flange and end-plate T-stubs

4.4 The tests results

In the following, the experimental results are reported and discussed. The detailed obtained results, in terms of load, displacements and collapse mode are reported in the Appendix A for each specimens. Also the bolts deformations and loads, as well as the related curves, are reported in the Appendix A (Paragraph 8).

4.4.1 The results of the tests on the end-plate T-stubs

The main results for each specimen, in terms of observed collapse modes and maximum load and displacement, are collected in Table 3. Although the measurements of the central transducer (i.e. transducer B) were usually employed for the force-displacement curves, the lateral transducers measurements (i.e. transducers A and C) permitted to monitor the specimen's behaviour. The lateral transducers measurements, not reported here, are collected in the experimental Appendix A. The relative difference between the measurements read by the lateral transducers, namely transducer A and C, is close to nil and the maximum displacement was usually measured by the central transducer. This behaviour justifies the crack opening at the centre of the weld toe and its progression to the plate edges.

END-PLATE T-STUBS				
Spec. ID	**Disp. rate** $\dot{\delta}$	**Maximum load**	**Displacement transducer B**	**Observed collapse mode**
	mm/s	kN	mm	
EP-01	326,90	331,37	15,81	1
EP-02	326,90	396,49	14,42	1
EP-03	326,90	347,27	21,22	1
EP-04	0,07	270,92	14,54	1
EP-05	0,07	302,67	21,60	1
EP-06	0,07	304,24	13,98	1
EP-07	160,00	321,68	13,04	1
EP-08	160,00	341,00	19,88	1
EP-09	160,00	324,57	15,36	1
EP-10*	160,00	335,10	22,26	1
*Snug tightened bolt				

Table 3: Tests results for the end-plate T-stubs

Figure 10 collects the photographs of an end-plate T-stub assembly (namely EP-09) during the test prior to the failure, and the T-stub specimen and the bolts after the collapse has occurred, as an example. The results obtained for each specimen are reported in the Appendix A.

In all the tests performed on the end-plate T-stub components, it was observed:

- the development of a clear flange mechanism independently of the deformation rate;
- the presence of cracks at the welds between the flange and the web;
- the failure of the bolts triggered by the development of cracks at the welds between the flange and the web;
- a collapse mode compatible with a mode type 1, amongst the collapse modes identified according to the Eurocode [21] (Table 1).

Specimen during the test

Specimen after the collapse

Bolt EP-09 A after the collapse

Bolt EP-09 B after the collapse

Figure 10: Test results for the specimen EP-09

The results of the tests in terms of load vs. flange displacement curves are reported in Figure 11. It permits the comparison between the curves of all the end-plate T-stubs tests (except for the specimen EP-10, discussed below), accounting for the different displacement rates. The comparison between the curves shows a moderate influence of the deformation rate on both the collapse load and the ductility of the tested specimens. This conclusion is in agreement with the findings of Pereira [7]. Concerning the EP-02 specimen, its behaviour (represented by the higher curve in the graph) deviates from the response of the other specimens, probably because of the specific mechanical characteristics of the welds between the flange and the web. Although the preliminary geometrical measurements didn't remark any anomaly, the analysis of the specimen collapse pointed out that the sudden failure of the weld between the flange and the web has triggered the collapse, without any previous detectable crack.

Figure 11 reports also the value of the collapse load evaluated according to the Eurocode formulation [21]. The design resistance here represented was calculated considering the mean geometrical and mechanical characteristics of the experimental assemblies and using the so-called method 1. The comparison between the curves shows that the calculated collapse load is in any case minor than the experimental values and is therefore widely conservative.

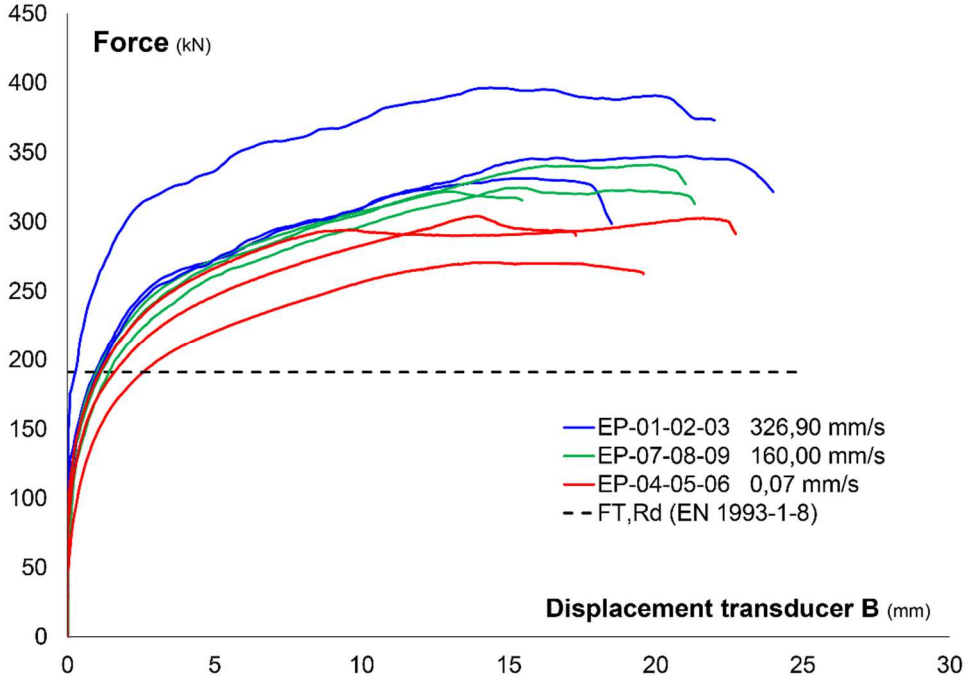

Figure 11: Comparison between tests results on the end-plate T-stubs

Figure 12 collects all the curves obtained testing the specimens with a loading rate of 160 mm/s. Also the curve related to the specimen EP-10 is reported, being the test carried out without bolt preloading. The negligible influence of the preloading can be observed.

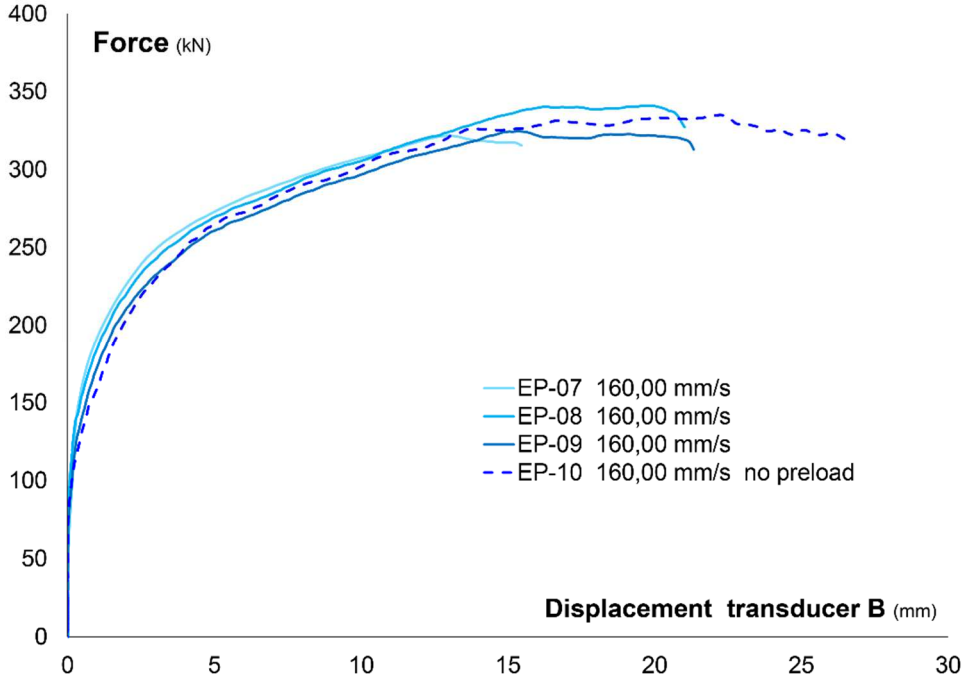

Figure 12: End-plate tests results, with a loading rate of 160 mm/s

4.4.2 The results of the tests on the column flange T-stubs

The results obtained testing the column flange T-stubs are gathered in Table 4 and Figure 13. Specimen C-04 was used to check the testing set-up, therefore the related results are not included.

COLUMN FLANGE T-STUBS				
Spec. ID	**Disp. rate $\dot{\delta}$**	**Maximum load**	**Displacement transducer B**	**Observed collapse mode**
	mm/s	kN	mm	
C-01	326,90	487,95	8,15	2 (3)
C-02	326,90	502,99	malfunction	2 (3)
C-03	326,90	510,92	9,40	2 (3)
C-04			Preliminary test	
C-05	0,07	458,42	11,84	2 (3)
C-06	0,07	441,19	8,33	2
C-07	0,07	465,53	7,27	2 (3)
C-08	160,00	445,35	6,84	2 (3)
C-09	160,00	487,30	6,82	2 (3)
C-10	160,00	479,81	6,61	2 (3)

Table 4: Tests results for the column flange T-stubs

Figure 13 permits the comparison between the experimental outcomes and the value of the collapse load evaluated using the Eurocode [21], calculated considering the mean geometrical and mechanical characteristics of the experimental assemblies. The calculated value is minor of the experimental collapse loads, even though the gap between the values is smaller than the one observed in the case of the end-plate T-stubs.

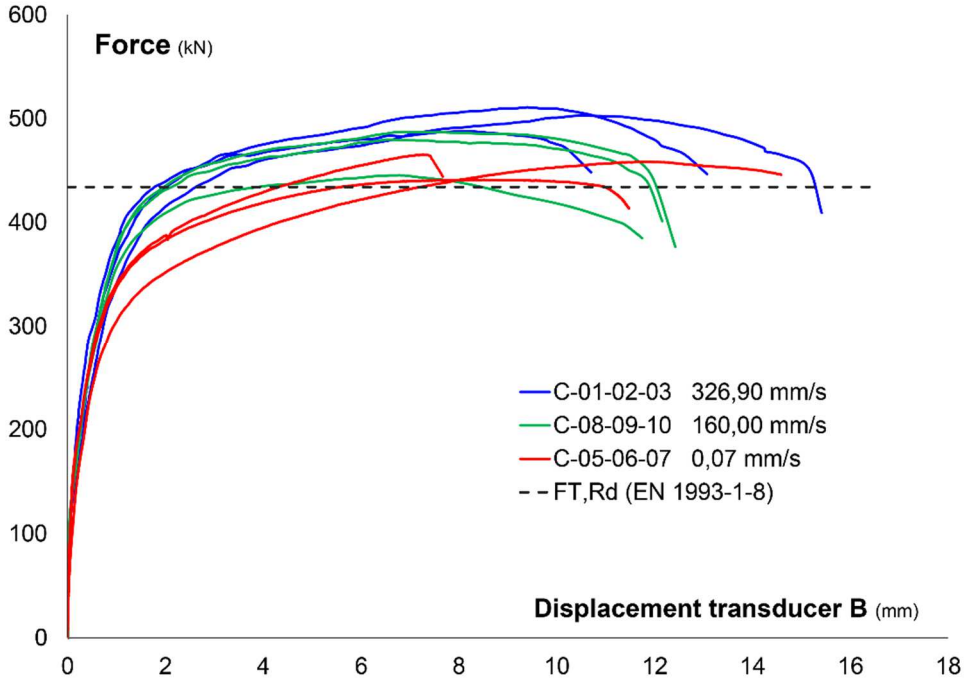

Figure 13: Comparison between tests results on the column flange T-stubs

Figure 14 collects the photographs of a column flange T-stub assembly (namely C-05) during the test and after the failure has occurred, as an example of the experimental outcomes.

Specimen during the test

Specimen after the collapse

Bolt C-05 A after the collapse

Bolt C-05 B after the collapse

Figure 14: Test results for specimen C-05

In all the column flange tests, it was observed:

- the partial development of a flange mechanism, which appeared more pronounced in tests performed at the lower deformation rate, i.e. the quasi-static tests (0,07 mm/s);
- the failure associated with the fracture of the bolts;
- a collapse mode compatible with a collapse mode identified as type 2, which was the collapse mode identified by the Eurocode [21] (Table 1). In most cases, the observed collapse mode was intermediate, not univocally classifiable as mode 2, but tending to mode 3 (as reported in the last column of Table 4).

The comparison between the force vs. flange displacement curves (Figure 13) seems to indicate a moderate influence of the loading rate on the collapse load. The lower collapse loads were observed in the quasi-static tests (0,07 mm/s). Furthermore, it appears that collapse loads are not affected by the displacement rate when the two higher values are compared (326,90 mm/s and 160 mm/s). It could be argued that a limit loading rate value exists and that when this limit is exceeded the influence of the loading rate on the maximum load is restricted. Nevertheless the limited number of performed tests and considered displacement rates prevents from getting general conclusions.

4.5 Considerations on the prying forces

As previously stated, a strain-gauge was installed in every bolt shank and each instrument was calibrated. The installation of the strain gauges internal to the bolts permitted to obtain the load vs. axial deformation and load vs. axial load relations for each bolt. An example of the curves obtained for the bolts during a T-stub test is shown in Figure 15, while the curves related to each specimen are gathered in Appendix A (Paragraph 8). The curves were dashed after the nominal yield point, since the bolts were calibrated in the

elastic range. The strain limit given by the strain gauge manufacturer ($4500x10^{-6}$ μm/m) is indicated by the vertical dashed line.

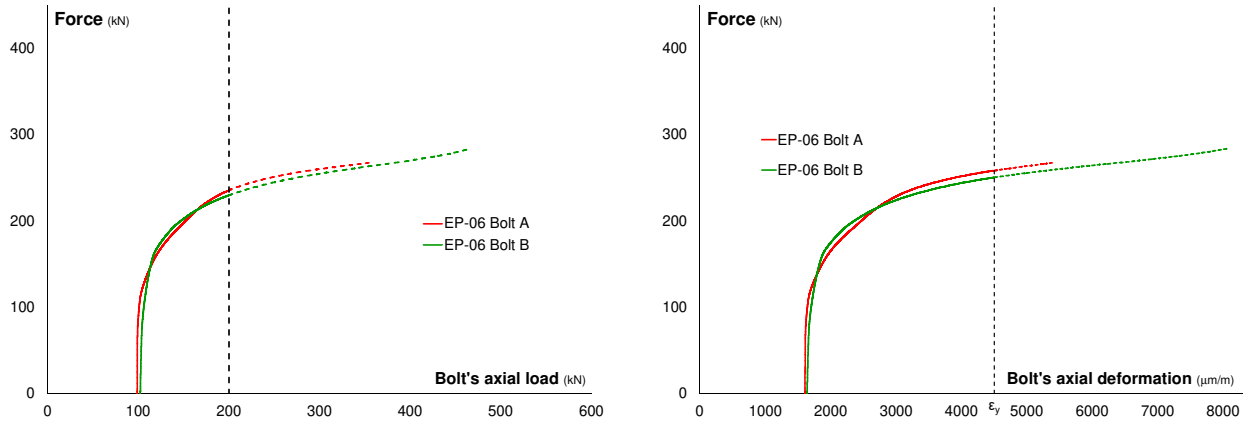

Load vs. bolt axial deformation *Load vs. bolt axial load*

Figure 15: Load vs. axial behaviour of the bolts (EP-06 bolts A and B)

The equilibrium conditions (Figure 2) enable computing the values of the prying forces when the axial loads acting in the bolts are known. It should be noticed that the instrumentation did not allow to have a reliable assessment of the prying forces at collapse. They were hence computed at the end of the elastic phase. Because of the unavoidable experimental asymmetries (see also Figure 15), the two prying forces are the same for each side of the T-stub. The mean values are considered. For the column flange T-stubs, characterized by collapse mode 2 (frequently close to mode 3), the forces were, on average, equal to less than 20% of the applied load. For the end-plate T-stubs, characterized by collapse mode 1, the forces were, on average, about 40% of the applied load. These values are in reasonable agreement with the literature, which reports mean values of the prying forces of about 30% of the applied load.

4.6 Discussion of the experimental results

Considering the whole set of tests, both on the column flange and end-plate T-stubs components, it was pointed outwhat follows:

- the potential influence of the deformation rate on the collapse load;
- the negligible influence of the deformation rate on the joint components ductility;
- the possibility of referring to the collapse modes identified by EN 1993-1-8 [21], and reported in Table 1, also in case of higher deformation rates;
- the possibility of referring to the collapse loads identified by EN 1993-1-8 [21] also in case of higher deformation rates, although rather conservatives;
- the importance of the quality of the welds between flange and web to prevent brittle failures.

The results obtained in this study are consistent with the findings of Pereira [7] and Pereira et al. [29]. Barata et al. [30] experimentally observed a slight increase of resistance with the increase of the loading rate. Also the specimens analysed in the present document, showed this slight increase of resistance.

In contrast with the study presented in this document, Barata et al. [30] observed that impact tests reach higher values of resistance for lower displacements, than those observed under quasi-static loading. In addition, the loading rate influence on the T-stubs response seems to be smaller for the tests reported in this

document if compared with the outcomes of Barata et al.. Nevertheless the limited number of tests and the different loading conditions prevent from getting general conclusions.

5 The numerical analysis

A FE analysis of the T-stubs was performed, developing some numerical models and calibrating them against the experimental results. The commercial software *Abaqus v.6.14* [10] was used for the analysis. Both the column flange and the end-plate T-stubs were modelled, and both quasi-static and dynamic simulations were performed, to be in compliance with the experimental programme.

The T-stubs performance involves a 3D highly nonlinear behaviour, characterized by complex phenomena as materials plasticity, second order effects and interaction problems. As a consequence, the numerical models have to account for them properly [33].

The simulations of the end-plate and the column flange T-stubs tensile tests were carried out in the same way. Therefore the description of the models and the simulations presented hereafter is applicable for both specimen types; otherwise it will be pointed out.

5.1 The description of the finite element models

All the simulations were carried out in large displacements taking into account mechanical and geometrical nonlinearities.

Taking advantage of the geometrical and loading symmetry, only half of the specimen was modelled, reducing the model complexity and saving computational time. The middle plane of the T-stubs web was identified as plane of symmetry of the assembly.

Each model was composed of six parts: the rigid support, the T-stub, the bolt, the nut and the washers. These parts were defined taking into account the average dimensions of the actual specimens, as determined in the experimental phase.

A particular attention was paid to the modelling of the bolt assembly, since experimentally the failure of the bolts was observed in the majority of the tests. The bolt thread wasn't modelled directly, therefore the thread presence was considered reducing the diameter of the bolt shank so as to obtain the nominal area of the bolt. This simplification permitted to consider the difference of stiffness and strength between the threaded and the unthreaded parts of the shank. As a consequence, also the nut diameter was reduced in order to maintain a perfect coupling between the two parts. The nut and the bolt were coupled using a "tie" constraint so they could behave as a single solid element. In order to make the model simpler, the bolt head and the nut were modelled as circular and also the unnecessary details of the bolts and nuts were removed. The washers were assembled with the bolt and the nut, paying particular attention to the definition of the interaction properties and the contact surfaces, as specified in the following.

The stress-strain relationships for the different materials were defined as follows. In the models, four different material laws were introduced: one for the T-stub, one for the bolt, one for the washers and one for the rigid support. Simplified elasto-plastic bilinear stress-strain relationships were adopted for the materials of the rigid support and the washers, due to their limited influence on the global assembly behaviour (Figure 16). On the contrary, the mechanical characteristics of the steel of both the T-stub and the bolt as obtained from the complementary tensile tests were adopted, being their correct characterization paramount for the precision of the analysis outputs. The stress-strain curves introduced to define the T-stub structural steels (both for the end-plate and the column flange T-stubs) were the true stress–true strain relationships obtained

experimentally (Figure 18). The bolt stress-strain relationship (Figure 17) was obtained experimentally through the tensile tests of the bolt assemblies and was verified and calibrated using a bolt, nut and washers assembly submodel. Indeed, in order to verify the correctness of the materials curves introduced in the analysis, single models of both the bolt's assembly and the steel coupons were developed and verified against the experimental outcomes.

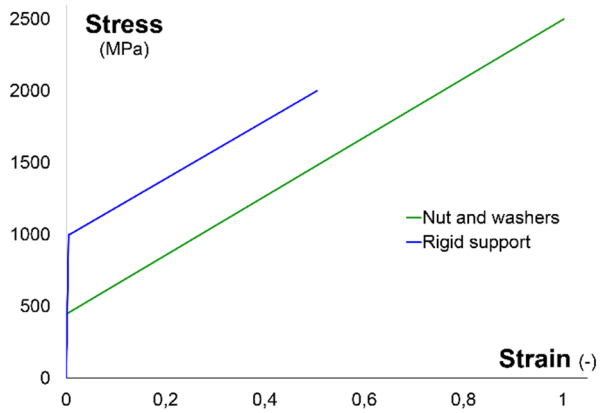

Figure 16: Washer, nut and rigid support stress-strain relationships introduced in the numerical models

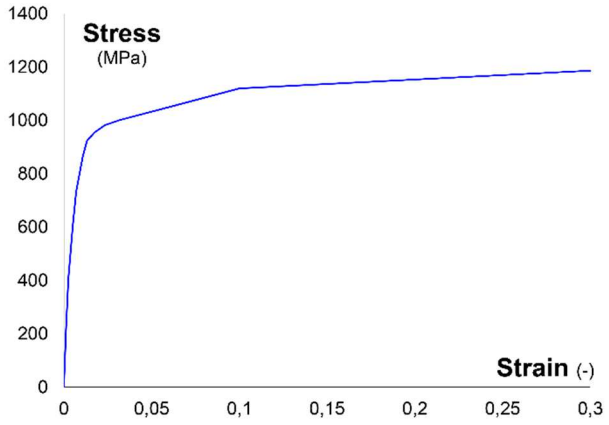

Figure 17: Bolt stress-strain relationship introduced in the numerical models

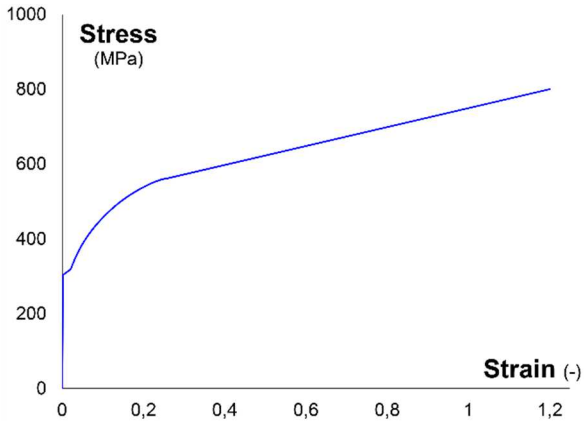

End-plate steel

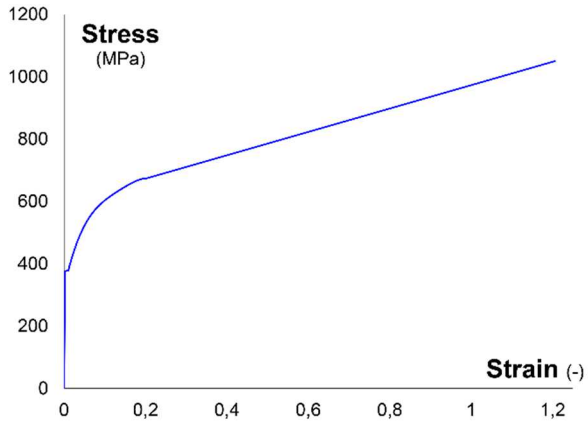

Column steel

Figure 18: T-stubs material stress-strain relationships introduced in the numerical models

The numerical analysis of the structural elements subjected to higher loading rates needs the definition of constitutive laws representing the behaviour of materials for a range of strain rates. In order to consider the strain rate influence on the materials behaviour, the Cowper-Symonds relation for structural steel was used (Paragraph 3.3.1). The parameters were defined on the basis of the experimental investigation carried out on the steel coupons. For the structural steel of the column flange T-stub $q = 3{,}44$ and $D = 473\ s^{-1}$ were calculated, while for the structural steel of the end-plate T-stub $q = 5$ and $D = 1130\ s^{-1}$ were obtained. To take into account the bolts behaviour at elevate strain rates, a dynamic increase factor was introduced, according to the results of the bolt assemblies tensile tests. The dynamic increase factor (DIF) is given by the relation of the dynamic yield strength σ_{dyn} to the yield strength obtained under static conditions σ_y: $DIF = \sigma_{dyn}/\sigma_y$. The DIF experimentally obtained for the bolts was equal to $1{,}05$.

A failure criterion based on continuum damage mechanics was introduced both for the bolt and the structural steel. The onset of the damage and the damage evolution are predicted following the formulation proposed by Hooputra et al. [34] included in the software *Abaqus* [10]. The damage parameters of the ductile damage model of the bolt and the structural steel (only for the material of the end-plate T-stub) were calibrated on the basis of the experimental outcomes. In particular, the damage parameters of the bolt were calibrated taking advantage of the submodel developed preliminary for the single bolt assembly. The damage parameters of the structural steel of the weld and of the material located in the nearness of the weld of the end-plate were instead calibrated using the whole model, since the single steel coupons experimentally tested were not welded, and so the mechanical characteristics of the welded zones couldn't be calibrated against the results of the single coupons tests. In the FE models the element deletion technique was also employed, allowing the removal of the finite elements from the mesh as they achieve a determinate value of damage. Hooputra et al. [34] advise that the procedure is suitable to predict crack initiation zones, although element removal should be regarded only as preliminary assessment for crack propagation simulation.

Each part of the assembly was modelled using 3D first order solid elements with eight nodes and reduced integration, type C3D8R, and allowing the introduction of the "enhanced hourglass control". Particular attention was paid to the model mesh definition, being the model highly mesh-sensitive. For the mesh of the bolt, the rigid support and the T-stub, a "structured" mesh with "Hex" element shape was implemented, while a "swept" mesh with "medial axis algorithm" was used for the nut and the washers. The mesh of the two FE models is represented in Figure 19. The choice of the dimensions of the finite elements was such that their number on the flanges thickness and in the bolt was adequate for an accurate description of the stress and strain fields. A discretization of 6 and 9 elements through the thickness of the flange was chosen for the end-plate and the column flange, respectively.

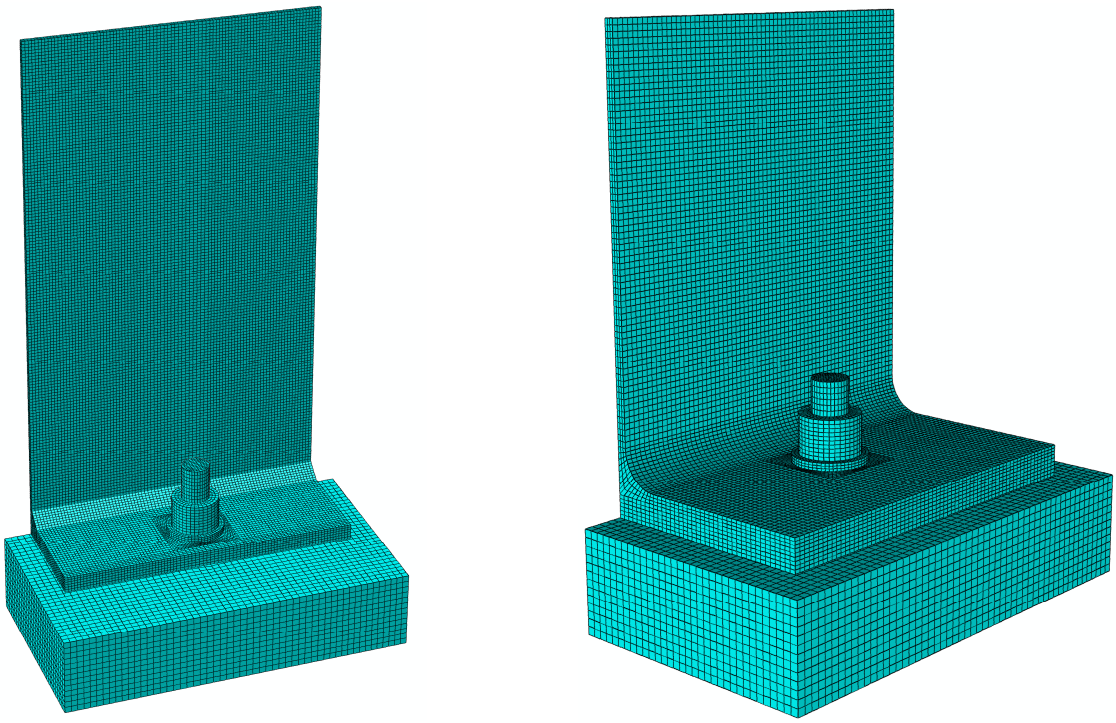

End-plate T-stub model *Column T-stub model*

Figure 19: Models mesh definition

The mesh density was increased in the zones where high stress concentrations were expected: more refined meshes were employed in the area of the T-stub flange around the bolt, in the bolt shank subjected to bending and in the weld line (for the end-plate T-stubs). The employed mesh refinements are represented in Figure 20. The selected solutions in terms of mesh density and elements dimensions are the result of an optimization process aimed at achieving balance between the number of nodes (and therefore the computational time) and the outcomes accuracy.

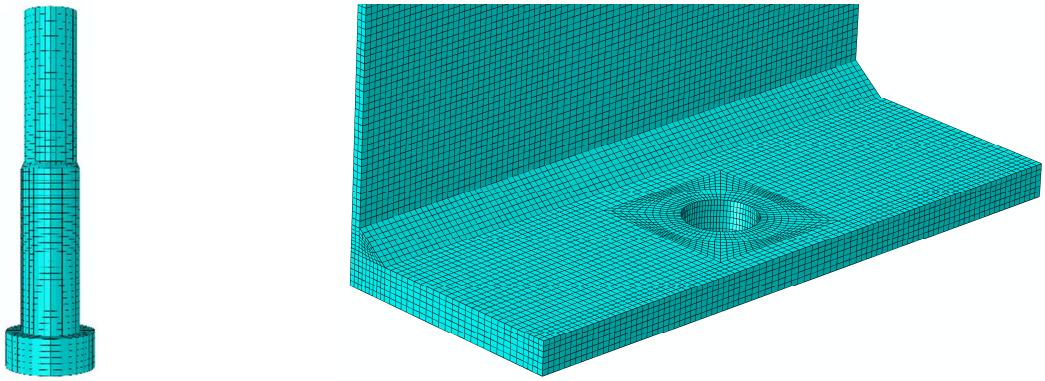

Bolt *Proximity to the flange bolt hole and end-plate weld*

Figure 20: Details of the mesh refinements

Since only half of the assembly was modelled, a symmetry boundary condition was introduced, providing the global equilibrium. Also a fixed boundary condition was assigned to the rigid support, simulating the rigid frame contribution (Figure 21).

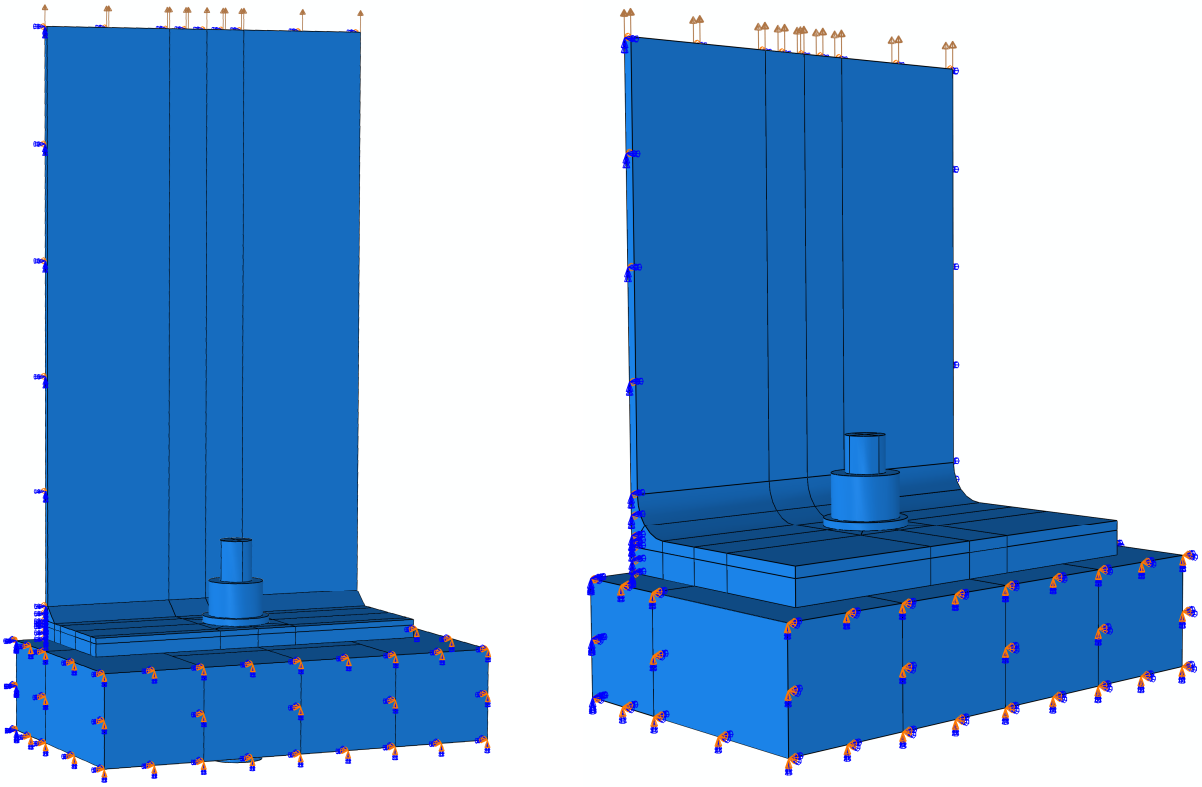

End-plate T-stub model *Column T-stub model*

Figure 21: Boundary and loading conditions

Two different analyses were performed in order to account for the bolt preloading and the following application of the tensile force. The bolt preload was simulated in a standard type of analysis, whose results were assumed as the initial state of the subsequent explicit analysis in which the tensile load was applied. Subsequently, an explicit analysis permitted to simulate the tensile phase of the tests, taking account of the dynamic contribution when necessary. The definition of the parts and the assembly remained the same in both of the analyses, while the interactions and the boundary and loading conditions were redefined in the model used for the explicit analysis. The use of the explicit method of analysis, instead of an implicit one, allowed to avoid convergence problems, especially in the case of a high number of degrees of freedom and nonlinearities caused by interaction problems.

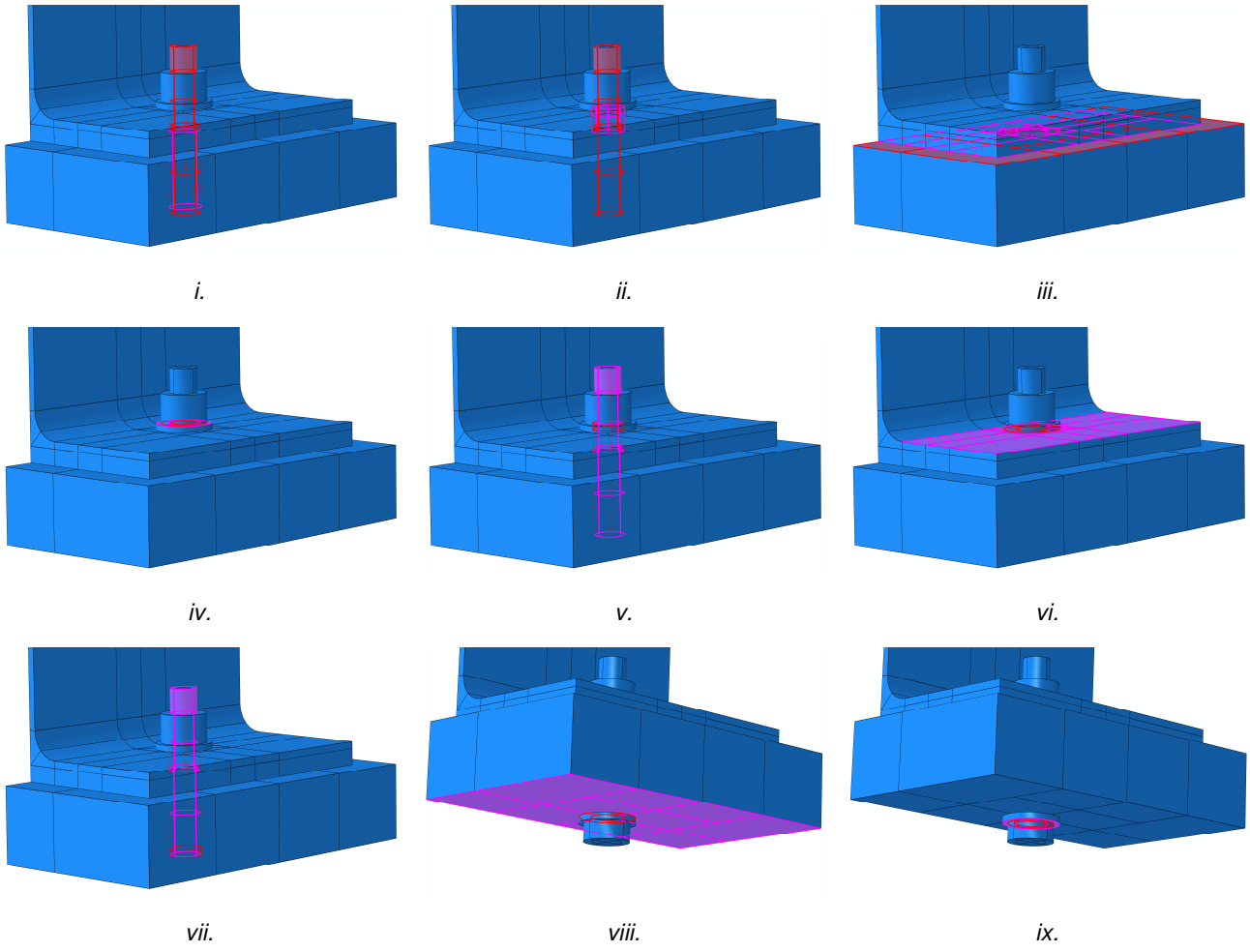

Figure 22: Contacts definition

Totally nine pairs of contacts were introduced in each model, as depicted in Figure 22.

The contact conditions were modelled between the following surfaces:

i. bolt shank and internal surface of the rigid support bolt hole;
ii. bolt shank and internal surface of the T-stub bolt hole;
iii. rigid support upper surface and T-stub lower surface;
iv. nut lower surface and upper surface of the top washer;
v. bolt shank and top washer internal surface;
vi. lower surface of the top washer and T-stub upper surface;

vii. bolt shank and bottom washer internal surface;

viii. upper surface of the bottom washer and rigid support lower surface;

ix. bolt head and lower surface of bottom washer.

The interactions between all the parts of the models were introduced by means of a surface-to-surface contact formulation. The formulation choice was made as a consequence of some preliminary numerical simulations that allowed to calibrate the contact parameters. In the standard simulation, a “penalty algorithm” with “friction coefficient” of 0,05 was introduced for the tangential behaviour, while normal contact behaviour was described by means of “hard contact” property with “penalty enforcement method”. In the explicit simulation, the same tangential behaviour was kept, while the normal behaviour was simulated with “hard contact” property and the default “enforcement method”. In both of the analyses, the surfaces separation after contact was allowed.

Concerning the loading application, in the standard analysis only the bolt preloading was applied, assigning a tensile action of 100 kN (calculated as the average value of the tensile loads applied experimentally) on an internal surface of the unthreaded part of the bolt shank (Figure 23). The stress field of the column flange T-stub assembly at the end of the standard analysis, i.e. the preload phase, is reported in Figure 23 (only the column flange T-stub results are showed as an example).

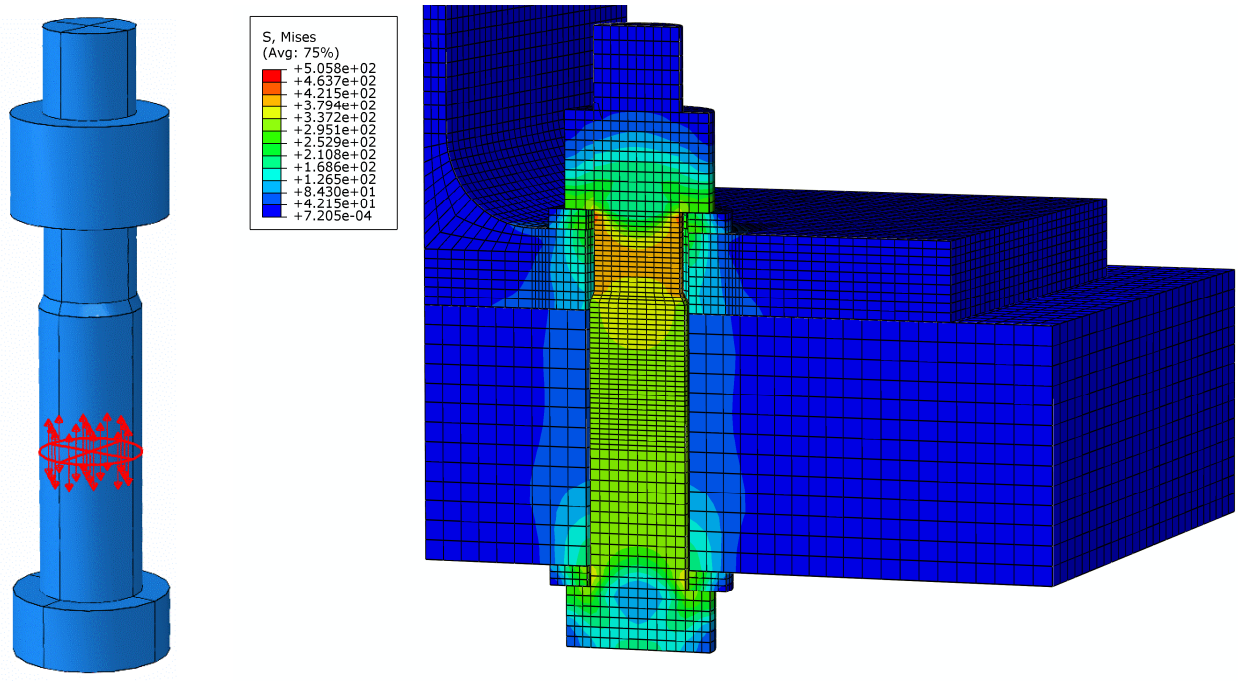

Figure 23: Preload application and stress field at the end of the standard analysis for the column flange T-stub

In the explicit analysis the tensile action on the web of the T-stub was assigned. In the quasi-static simulations the tensile action was set introducing a boundary condition type “displacement” with uniform distribution on the web of the T-stub, in order to simulate the displacement control loading protocol. In the dynamic simulations, a boundary condition type “velocity” was assigned to the web of the T-stub, introducing the experimental displacement rate value (Figure 21).

The feature of the end-plate T-stub model should be remarked. The end-plate T-stub was experimentally obtained through the welding of two separated flanges. In order to properly simulate this element, a unique part representing the T-stub and comprising the weld was modelled and a seam between the two flanges

was introduced. The weld was modelled as a triangular prism, whose dimensions were defined as the average values of the actual dimensions of the welds measured prior to the tests. The weld mechanical characteristics were assumed to be the same of the flanges, since in the experimental phase the actual mechanical characteristics of the weld weren't analysed in detail. The damage parameters of the material were then calibrated in order to account for the weld presence and the subsequent modification to the mechanical characteristics, as previously stated.

5.2 The comparison of the experimental and the numerical results

The validation of the numerical models was based on the experimental results. The overall responses, and specifically the deformed configurations, were primarily compared in order to verify the accuracy of the boundary conditions, the restraints arrangement and the loading application. The collapse modes were also evaluated and compared, considering the plastic hinges development, the bolt failure or the cracks presence in the weld (for the end-plate T-stubs). The load vs. displacement numerical curve was also evaluated and compared with the experimental curves, considering a reference point located as the displacement transducer B.

In Figure 24, Figure 25 and Figure 26, the comparison between the experimental and numerical results is presented for column flange T-stubs subjected to displacement rates of 0,07 mm/s, 160 mm/s and 326,00 mm/s respectively. Figure 27, Figure 28 and Figure 29 represent the end-plate T-stubs responses, when subjected to displacement rates of 0,07 mm/s, 160 mm/s and 326,00 mm/s respectively.

Considering the curves reported in Figure 29, it should be noticed that the experimental curve related to EP-02 (the higher curve in Figure 11) has been removed, due to its difference respect to the other curves, as pointed out in Paragraph 4.4.1. As a consequence, the numerical model was calibrated only on the basis of the other two curves, namely EP-01 and EP-03.

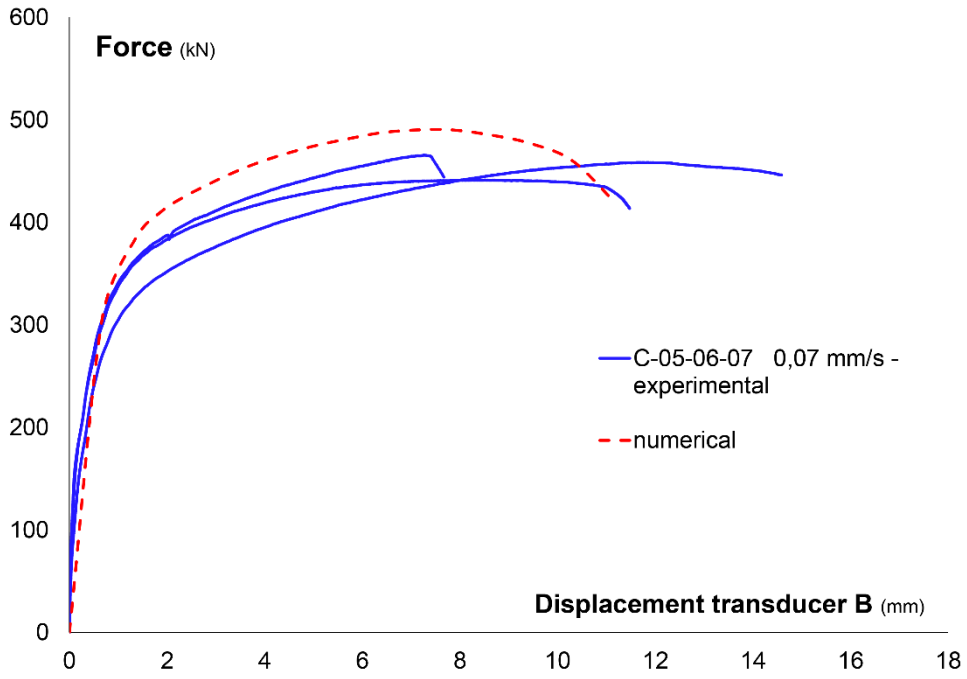

Figure 24: Comparison between experimental and numerical results for column flange T-stubs subjected to quasi-static tests (0,07 mm/s)

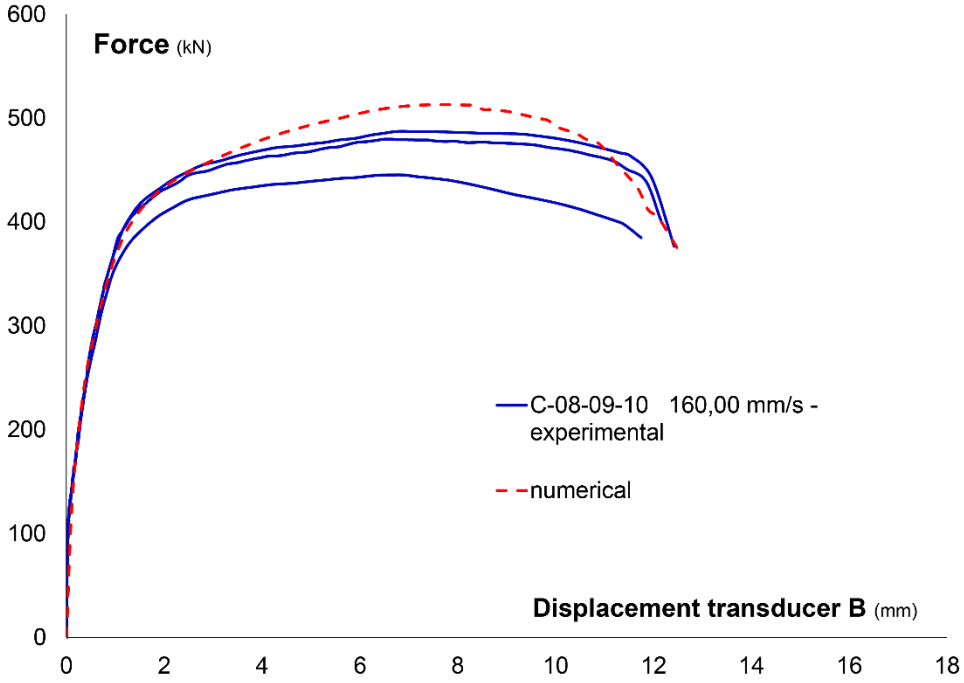

Figure 25: Comparison between experimental and numerical results for column flange T-stubs subjected to the intermediate displacement rate (160,00 mm/s)

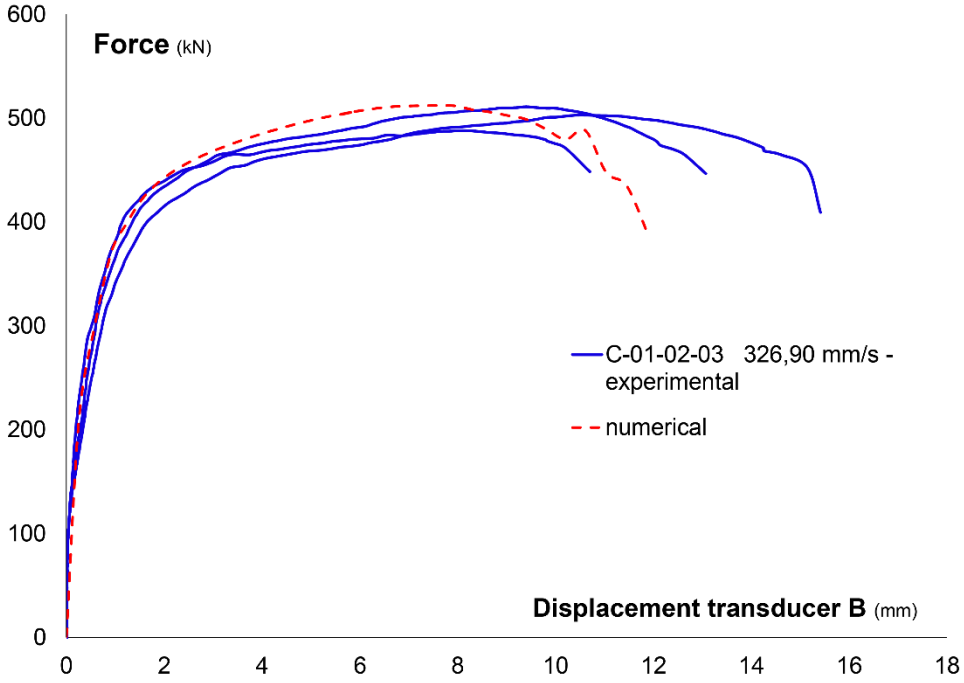

Figure 26: Comparison between experimental and numerical results for column flange T-stubs subjected to the higher displacement rate (326,90 mm/s)

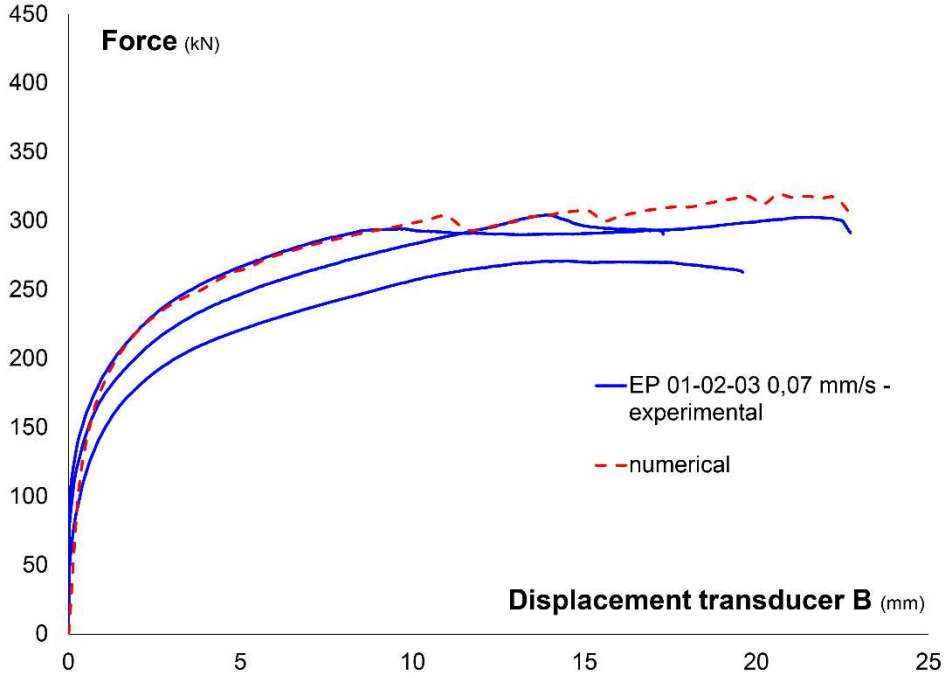

Figure 27: Comparison between experimental and numerical results for end-plate T-stubs subjected to quasi-static tests (0,07 mm/s)

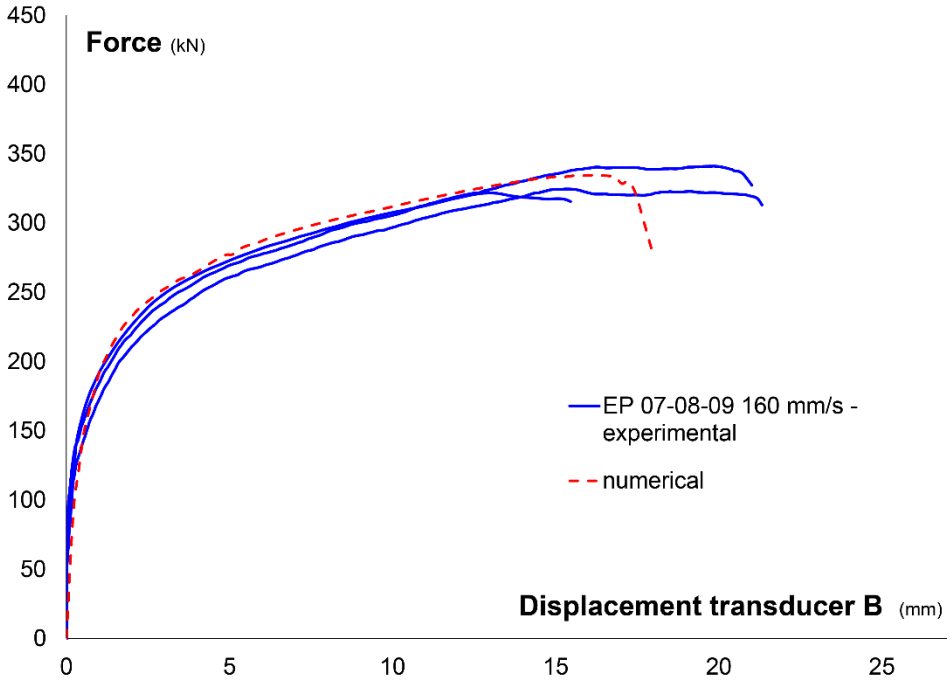

Figure 28: Comparison between experimental and numerical results for end-plate T-stubs subjected to the intermediate displacement rate (160,00 mm/s)

In Figure 30 the comparison between the experimental and numerical results for the end-plate T-stubs at a displacement rate of 160 mm/s are collected, considering both of the cases of preloaded bolts and snug tightened bolts. In agreement with the experimental observations, the numerical model predicts the negligible influence of the preloading.

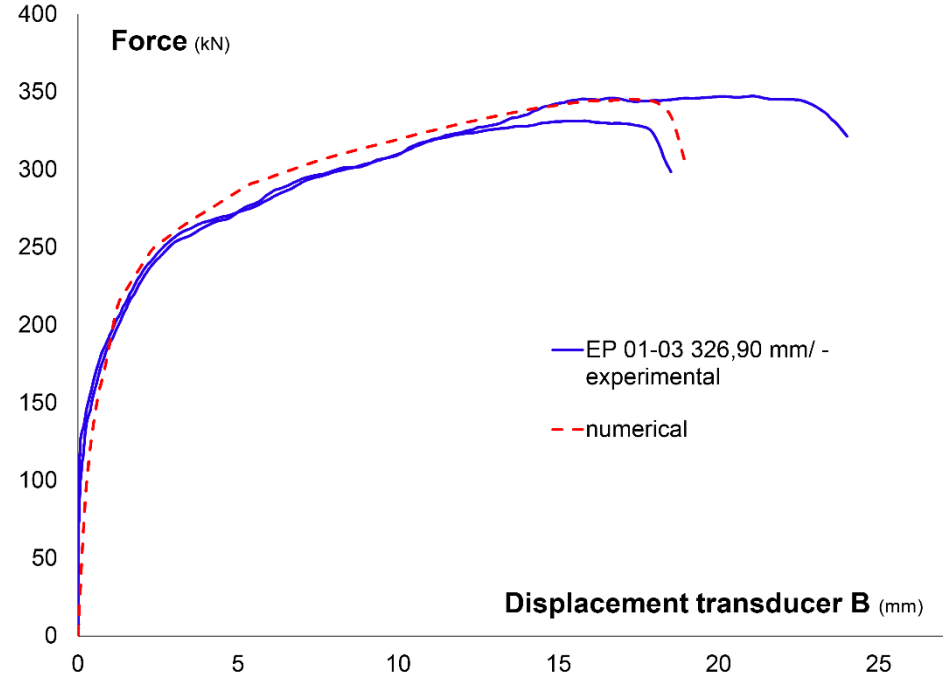

Figure 29: Comparison between experimental and numerical results for end-plate T-stubs subjected to the higher displacement rate (326,90 mm/s)

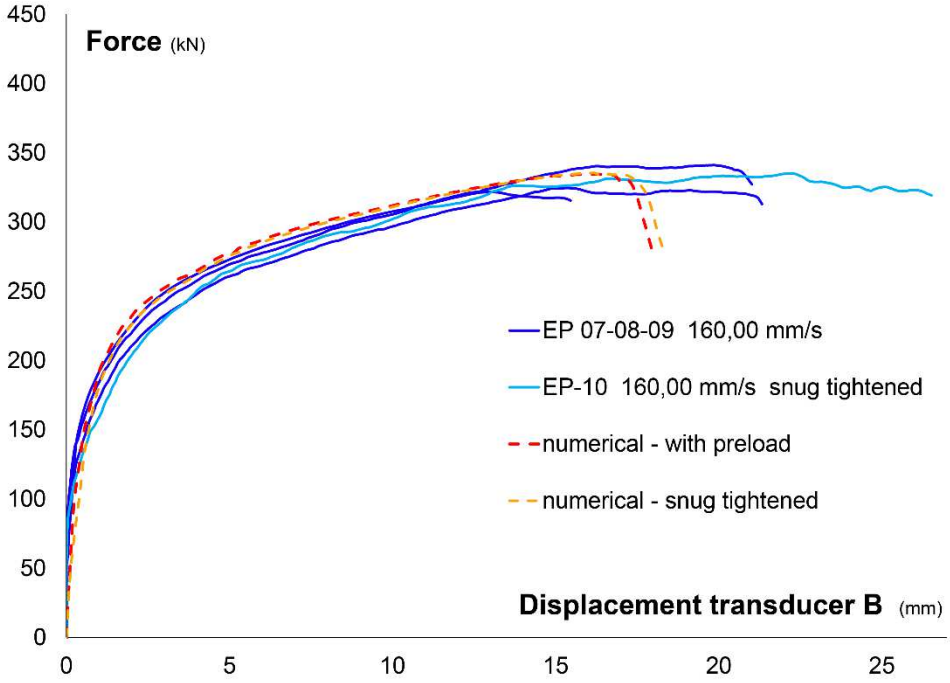

Figure 30: Comparison between experimental and numerical results for end-plate T-stubs subjected to the intermediate displacement rate (160,00 mm/s), with applied preload and snug tightened bolts

The agreement between the tests results and the numerical simulations outcomes is quite satisfactory in terms of collapse loads and modes both for the column flange and the end-plate T-stubs. The numerical model predicts the overall behaviour of the T-stubs assemblies during all the test phases.

As previously pointed out, the numerical and experimental results can also be compared qualitatively, in terms of deformed shape, plastic hinges localization and elements failure (Figure 31 and Figure 32).

Concerning the column flange T-stubs, the failure is driven by the bolt, whose behaviour and damage were modelled through the introduction of a damage law, calibrated on the basis of the bolt submodel developed and validated against the experimental results of the tensile tests of the single bolt assemblies.

The end-plate T-stubs failure is, on the contrary, controlled by the failure of the end-plate near the weld toe, both experimentally and numerically. The numerical model can successfully predict the development of the cracking in the end-plate weld using the defined failure criterion (Figure 32).

The accuracy of the results already enables some parametrical analyses needed to improve the connection design.

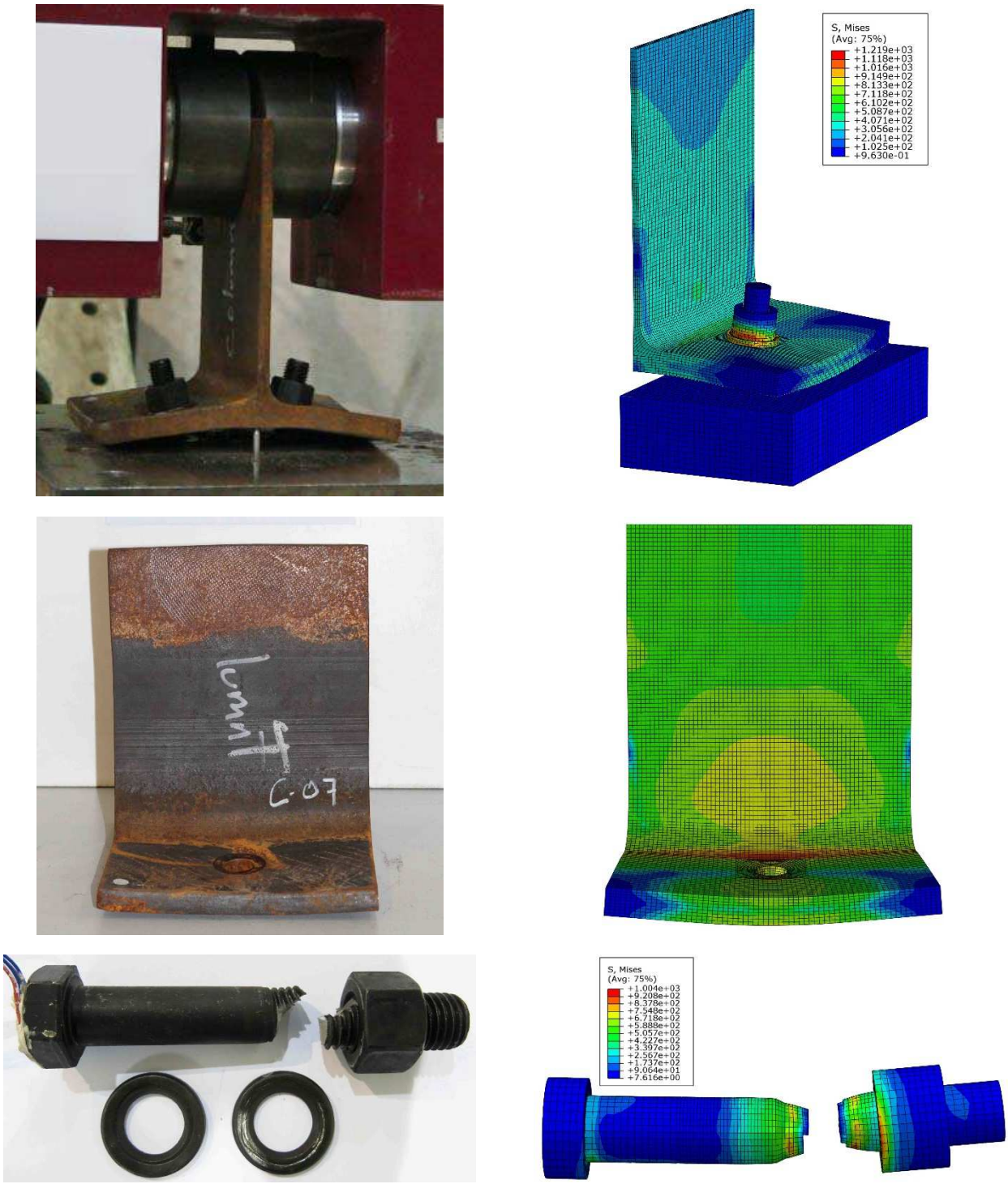

Figure 31: Qualitative comparison of the experimental and the numerical results for the column flange T-stubs

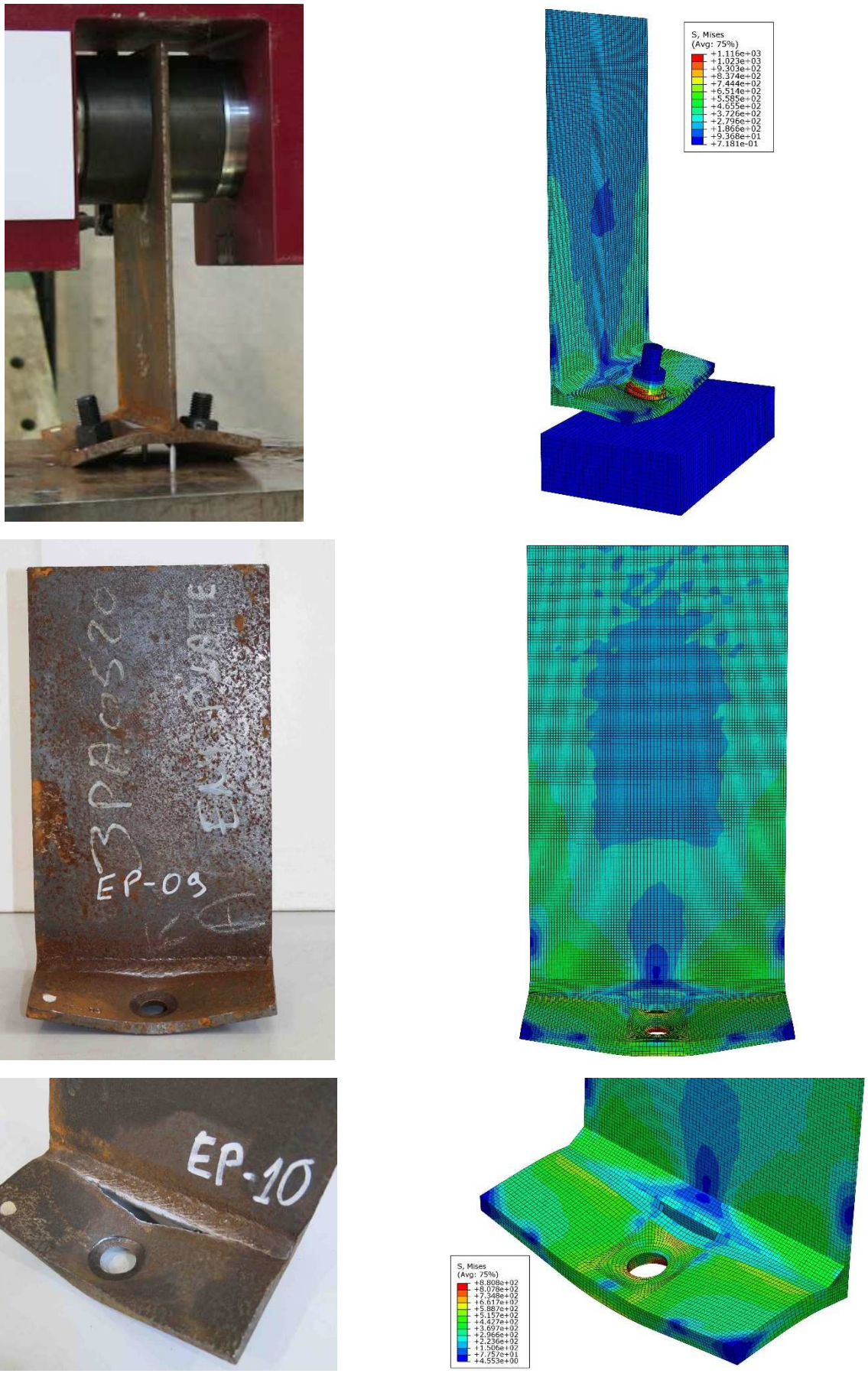

Figure 32: Qualitative comparison of the experimental and the numerical results for the end-plate T-stubs

6 Summary and conclusions

The experimental and numerical analyses performed on a series of T-stubs subjected to tensile loadings at different rates are reported in this document. The study is part of the European research project “RobustImpact” [8], and the T-stubs were representative of the end-plate beam-to column joints of the reference frames [8]. In the experimental phase, twenty tests were carried out: ten for the column flange and ten for the end-plate T-stub component. Two deformation rates were selected for the dynamic tests (160,00 mm/s and 326,90 mm/s), and quasi-static tests (0,07 mm/s) were carried out for comparison. The numerical models both of the column flange and the end-plate T-stubs were then developed, considering the mean values of the geometrical and mechanical characteristics of the tested specimens. The models incorporated the strain rate sensitivity and the damage evolution of the materials. In the document, the numerical results obtained from quasi-static and dynamic simulations are reported and compared with the experimental outcomes.

Despite the limited number of tests, this study provides an insight into the influence of the deformation rate on the collapse load and mode of the considered T-stubs. The results seem to indicate that the influence of the deformation rate on the tensile capacity of the T-stub is not significant, and that it is negligible on its ductility. In addition, it seems that the collapse modes and loads determined in accordance with the Eurocode [21] can be referred to also in case of higher deformation rates. Finally, the importance of the quality of the weld between flange and web was pointed out, both by the experimental and by the numerical analyses.

7 Bibliography

[1] Kuhlmann, U., Rölle, L., Jaspart, J.-P., Demonceau, J.-F., Vassart, O., Weynand, K., Ziller, C., Busse, E., Lendering, M., Zandonini, R., Baldassino, N., *Robust structures by joint ductility*, Contract No RFSR-CT-2004-00046, Report EUR 23611 EN, European Commission, RFCS Research, - ISBN 978-92-79-10360-5, Brussels, 2009

[2] Zoetemeijer, P., *A design method for the tension side of statically loaded, bolted beam-to-column connections*, Heron - Stevin Laboratory, vol. 20 (1), Delft, The Netherlands, 1974

[3] Jaspart, J.-P., *Etude de la Semi-Rigidite des Noeuds Poutre-Colonne et son Influence sur la Resistance et la Stabilite des Ossatures en Acier*, Ph.D. Thesis, Department MSM, University of Liège, Belgium, 1991

[4] Faella, C., Piluso, V., Rizzano, G., *Structural steel semirigid connections: theory, design and software*, Boca Raton, Fla.: CRC press LLC, 2000

[5] Cowper, G. R., Symonds, P. S., *Strain-hardening and strain-rate effects in the impact loading of cantilever beams*, Technical Report No. 28, Division of Applied Mathematics, Brown University, Providence, 1957

[6] Johnson, R. G., Cook, W. H., *A constitutive model and data for metals subjected to large strains, high strain rates and high temperature*, in Proceedings of the 7th International Symposium on Ballistics, 19-21 April, the Hague, Netherlands, Seventh International Symposium on Ballistics, 1983

[7] Pereira, M., *Robustness of multy-storey steel-composite buildings under column loss: rate-sensitivity and probabilistic framework*, Ph.D. Thesis, Department of Civil and Environmental Engineering, Imperial College London, 2012

[8] Kuhlmann, U., Hoffmann, N., Jaspart, J.-P., Demonceau, J.-F., Zandonini, R., Baldassino, N., Hoffmeister, B., Colomer, C., Korndörfer, J., Hanus, F., Charlier, M., Hijaj, M., Gueouli, S., *Robust impact design of steel and composite building structures (ROBUSTIMPACT)*, Final Report, Contract No RFSR-CT-2012-00029, Report EUR 28578 EN, European Commission, RFCS Publications, - ISBN 978-92-79-68610-8, Brussels, 2017

[9] Baldassino, N., Bernardi, M., Zandonini, R., *Study of the loading rate influence on the T-stub response,* in Institut für Konstruktion und Entwurf Universität Stuttgart (edited by), Stahlbau, Holzbau und Verbundbau, Festrschrift zum 60. Geburtstag von Univ.-Prof. Dr.-Ing. Ulrike Kuhlmann, - ISBN: 978-3-433-03246-6, Berlin: Ernst & Sohn, 2017, p. 182-187

[10] Abaqus 6.14 Online Documentation © Dassault Systèmes, 2014 http://50.16.225.63/v6.14/ , 2017 (accessed 03/08/17)

[11] Haberland, M., Starossek, U., *Progressive collapse nomenclature*, ASCE SEI 2009 Structures Congress: Don't Mess with Structural Engineers, Austin, Texas, April 29-May 2009, ASCE/SEI (2009), pp. 1886–1895

[12] Starossek, U., Progressive collapse of structures: nomenclature and procedures, *Structural Engineering International,* 2/2006, pp. 113–117

[13] Consiglio Superiore dei Lavori Pubblici, *Norme Tecniche per le Costruzioni D.M. 14 gennaio 2008 e Circolare applicativa 2 febbraio 2009 n. 617 - Istruzioni per l'applicazione delle "Nuove norme tecniche per le costruzioni" di cui al D.M. 14 gennaio 2008*

[14] HM Government: Building Regulations 2010 – Structure - *Approved Document A*, NBS, London 2004

[15] ASCE/SEI 7-10: *Minimum Design Loads for Buildings and Other Structures*, Reston, Virginia, 2013

[16] EN 1991-1-7:2014. *Eurocode 1: Actions on structures. Part 1-7: General actions - Accidental actions*, CEN European Committee for Standardization, 2014

[17] Iding, R., *A Methodology to Evaluate Robustness in Steel Buildings — Surviving Extreme Fires or Terrorist Attack Using a Robustness Index*, in Structures Congress 2005: Metropolis and Beyond, April 20-24, New York, edited by ASCE, Reston, 2005, pp. 1-5

[18] Ellingwood, B. R., Dusenberry, D. O., Building Design for Abnormal Loads and Progressive Collapse, *Computer-Aided Civil and Infrastructure Engineering*, 20 (2005), pp. 194-205

[19] EN 1993-1-1, *Eurocode 3 Design of steel structures – Part 1-1: General rules and rules for buildings*, CEN European Committee for Standardization, 2005

[20] EN 1994-1-1, *Eurocode 4 Design of composite steel and concrete structures – Part 1-1: General rules and rules for buildings*, CEN European Committee for Standardization, 2005

[21] EN 1993-1-8, *Eurocode 3 Design of joints – Part 1-8: Design of joints*, CEN European Committee for Standardization, 2005

[22] Yee, Y. L., Melchers, R. E., Moment rotation curves for bolted connections, *Journal of Structural Engineering*, vol. 112 (3) (1986) pp.615-635

[23] Arup, *Review of international research on structural robustness and disproportionate collapse*, Department for Communities and Local Government, London, 2011

[24] Jones, N., *Structural impact*, Cambridge University Press, New York, 2011

[25] Jones, N., The credibility of predictions for structural designs subjected to large dynamic loadings causing inelastic behaviour, *International Journal of Impact Engineering*, vol. 53 (2013) pp. 106-114

[26] Swanson, J. A., Leon, R. T., Bolted steel connections: tests on T-stub components, *Journal of structural engineering*, 126(1), (2000), pp.50-56

[27] Girão Coelho, A. M., Bijlaard, F. S. K., Gresnigt, N., da Silva, L.S., Experimental assessment of the behaviour of bolted T-stub connections made up of welded plates, *Journal of Constructional Steel Research* 60 (2004) pp. 269–311

[28] Bursi, O.S., Ferrario, F., Fontanari, V., Non-linear analysis of the low-cycle fracture behaviour of isolated Tee stub connections, *Computers and Structures,* 80 (2002), pp. 2333–2360

[29] Pereira, M., Izzudin, B. A., Baldassino, N., Zandonini, R., Buoso, F., Mancini, V., *Rate sensitive behaviour of bolted end-plate steel connections – an experimental and numerical assessment*, Internal Report, University of Trento and Imperial College London, 2012

[30] Barata, P., Santiago, A., Rodrigues, J. P. C., Rigueiro, C., *Experimental analysis of a T-stub component subjected to impact loading*, in Eurosteel 2014 : 7th European conference on steel composite structures : September 10-12, 2014 Naples, Italy, edited by R. Landolfo, F. M. Mazzolani, ECCS, Brussels 2014

[31] Ribeiro, J., Santiago, A., Rigueiro, C., Barata, P., Veljkovic, M., Numerical assessment of T-stub component subjected to impact loading, *Engineering Structures,* 106 (2016), pp. 450-460

[32] Baldassino, N., Bernardi, M., Zandonini, R., *T-stub response and loading rate*, in Connections VIII 8th International Workshop on Connections in Steel Structures, Editors: Charles J. Carter and Jerome F. Hajjar, AISC 2016 - ISBN: 978-1-56424-019-4. Proceedings of the Eighth International

Workshop on Connections in Steel Structures held at Hilton Boston Back Hotel, Boston, Massachusetts, USA, May 24-26, 2016

[33] Nethercot, D. A., Zandonini, R., *Methods of prediction of joint behaviour: beam-to-column connections*, in: R. S. Narayanan, Structural connections: stability and strength, Elsevier Applied Science Publisher, London, New York, 1989

[34] Hooputra, H., Gese, H., Dell, H., Werner, H., A comprehensive failure model for crashworthiness simulation of aluminium extrusions, *International Journal of Crashworthiness*, vol. 9 (5) (2004) pp. 449–464